

Alterations to the Membrane Properties of CA1 Pyramidal Neurons by the Amnestic Agent
Anisomycin

by

Michelle Jo-ann LeBlancq

A thesis submitted in partial fulfillment of the requirements for the degree of

Master of Science

Centre for Neuroscience
University of Alberta

© Michelle Jo-ann LeBlancq, 2017

Abstract

The notion that long-term memory is dependent upon the production of new proteins is a near-axiomatic assertion in the field of behavioural neuroscience. The idea that protein synthesis is required for long-term memory formation and maintenance is based largely on the amnesic effects of protein synthesis inhibitors such as anisomycin (ANI). One issue with this hypothesis, however, is that protein synthesis inhibitors have been shown to alter other aspects of neurobiological functioning. Previous work from our lab has shown an impairment of neural activity and functional integrity of the hippocampus following intracerebral infusions of ANI. We therefore sought to investigate how protein synthesis inhibition using ANI might affect passive and active membrane properties of hippocampal CA1 principal neurons. Firstly, we used radiolabelled amino-acid incorporation to confirm that a short (30 minute), low concentration (100 μ M) bath application of ANI to acute transverse hippocampal slices was sufficient to produce an inhibition of protein synthesis, and observed an approximately 45% decrease in amino acid incorporation. Secondly, bath application of anisomycin on CA1 pyramidal cells recorded via whole-cell patch-clamp configuration showed that ANI caused a reduction in membrane polarization and detrimentally affected firing properties, without any changes in input resistance, membrane time constant, or threshold to elicit an action potential. Lastly, this pattern of results suggested that anisomycin might be disrupting mitochondrial activity, which was confirmed using a marker of electron transport; 2,3,5-triphenyltetrazolium chloride (TTC). Overall, these findings further the knowledge of how agents such as ANI may produce impairments of neural activity (as well as amnesia), and extend caution toward the evaluation of behavioural responses to molecular manipulations without considering effects on cellular and network function in the nervous system.

Preface

This thesis is an original work by Michelle J. LeBlancq. The research project, of which this is a part, received research ethics approval from the University of Alberta Research Ethics Board, Project Name “Cellular and Network Dynamics of Neo- and Limbic-Cortical Brain Structures”, No. BS 606, exp. March 31, 2016.

Some of the research conducted for this thesis forms part of an internal research collaboration, led by Professor Clayton T. Dickson together with Professor Frank E. Nargang at the University of Alberta.

This thesis is an original work by Michelle J LeBlancq. No part of this thesis has been previously published.

Acknowledgements

Thank you to my supervisors Dr. Clayton Dickson and Dr. Trevor Hamilton. Thank you for the opportunities you have given me learning new techniques, travelling to conferences, and presenting my research.

Thank you to my supervisory committee Dr. Greg Funk and Dr. Declan Ali. Thank you both for your guidance, support, and criticism. Thank you for opening your labs to me in order to troubleshoot problems, as well as use equipment I did not have access to.

Thank you to Dr. Simon Gosgnach and John Misiaszek for acting as the arm's length examiner and chair for my thesis defence, and for your helpful comments.

Thank you to Dr. Frank Nargang for collaborating with us on the autoradiography experiments, and teaching me the techniques necessary to do so.

Thank you to Megan Airmet for your guidance and knowledge throughout my time in the program.

Thank you to the entire Brain Rhythms lab for making my grad school experience fun, both inside and outside the lab.

Thank you to my amazing friends and family for your support and love.

Table of Contents

Introduction.....	1
Memory	1
Protein Synthesis Inhibitors and Memory	3
Issues with the <i>de novo</i> hypothesis.....	6
Influence of PSIs on neural activity	8
Elucidation of a protein synthesis dependent depression of neural activity	10
Hippocampal Anatomy.....	10
CA1.....	11
Purpose	19
Materials and Methods.....	20
Preparations and Solutions	20
Electrophysiology.....	20
Autoradiography.....	23
Triphenyltetrazolium Chloride Staining.....	24
Statistical Analysis	24
Results.....	25
Bath application of ANI inhibits protein synthesis in hippocampal slices.....	25
ANI cause a loss of membrane potential without changing other passive membrane properties in CA1 neurons	25
ANI alters single action potential properties of CA1 neurons	31
ANI alters multi-spike characteristics in CA1 neurons.....	37
ANI reduces mitochondrial activity as evidenced by a decrease in TTC staining.....	45
Discussion.....	48
Electrophysiological properties of CA1 pyramidal neurons	48
The membrane effects of ANI are consistent with mitochondrial dysfunction	49
Effects of ANI on multiple spiking characteristics	50
Inhibition of protein synthesis in hippocampal slices	51
Effect of protein synthesis inhibition on other cell types.....	52
Effects of targeted molecular manipulations on neural activity.....	53
Effects of alterations of neural activity on memory	54
Conclusions	55
References	57

List of Tables

Table 1. Passive Membrane Properties	32
Table 2. Single Action Potential Active Membrane Properties	38
Table 3. Multiple Spike Properties	43

List of Figures

Figure 1. Stages of Memory.....	4
Figure 2. The Hippocampal Formation	13
Figure 3. Neural Connectivity in the Hippocampus	15
Figure 4. CA1 Pyramidal Cell Morphology and Synaptic Inputs.....	17
Figure 5. Anisomycin inhibits protein synthesis in hippocampal slices.....	26
Figure 6. Anisomycin significantly depolarizes CA1 cells, but does not change input resistance nor membrane time constant.....	28
Figure 7. Effect of ANI on single spike characteristics	35
Figure 8. Effect of ANI on other spiking characteristics	40
Figure 9. Anisomycin impairs mitochondrial activity	46

List of Symbols and Abbreviations

AC	Associational commissural pathway	SPRs	Sharp-wave ripples
aCSF	Artificial cerebral spinal fluid	s.r.	Stratum radiatum
AMPA	Alpha-amino-3-hydroxy-5-methyl-4-isoxazoleproponic acid	STM	Short-term memory
ANI	Anisomycin	τ	Membrane time constant; tau
ANOVA	Analysis of variance	T	Temporal cortex
AP	Action potential	TTC	2,3,5-triphenyltetrazolium chloride
ATP	Adenosine tri-phosphate	TTX	Tetrodotoxin
CA1	Cornu Ammonis 1	V	Voltage
CA2	Cornu Ammonis 2	V_m	Membrane voltage
CA3	Cornu Ammonis 3	ZIP	Zeta inhibitory peptide
cAMP	Cyclic adenosine monophosphate		
C_m	Membrane capacitance		
CREB	cAMP-responsive element binding protein		
DG	Dentate gyrus		
DPI	Dots per inch		
EC	Entorhinal cortex		
EEG	Electroencephalogram		
I	Current		
LEC	Lateral entorhinal cortex		
LFP	Local field potential		
LPP	Lateral perforant path		
LTM	Long-term memory		
LTP	Long-term potentiation		
mAHP	Medium after-hyperpolarization		
MEC	Medial entorhinal cortex		
MF	Mossy fibre pathway		
MPP	Medial perforant path		
NMDA	N-methyl-D-aspartate		
PKM ζ	Protein kinase M zeta		
PP	Perforant pathway		
PSI(s)	Protein synthesis inhibitor(s)		
R_{input}	Input resistance		
R_m	Membrane resistance		
RMP	Resting membrane potential		
S	Septal nuclei		
Sb	Subiculum		
SEM	Standard error measurement		

Introduction

Despite decades of research into the biological basis of learning and memory, researchers have not yet determined the exact mechanisms governing these complex processes. One major focus has been on changes in the molecular machinery involved in synaptic plasticity (Kandel, 2001), leading to the hypothesis that *de novo* protein synthesis is required for the maintenance of long-term memory (for review see (Davis and Squire, 1984). This theory has been supported by influential experiments using global protein synthesis inhibitors (PSIs) such as anisomycin (ANI; for review see (Kwapis and Helmstetter, 2014). A major problem with this line of evidence, however, is the fact that ANI and other PSIs might modify other aspects of neurobiological function that may or may not depend on protein synthesis (Cohen and Barondes, 1966, 1967; Dahl, 1969; Schwartz et al., 1971; Luttges et al., 1972; Wilcox et al., 1974; Kleim et al., 2003; Canal et al., 2007; Qi and Gold, 2009). In particular, our lab has recently shown that anisomycin impairs neural activity (Sharma et al., 2012) as well as the operational integrity of the hippocampus (Greenberg et al., 2014; Dubue et al., 2015). A major question remaining is how ANI might affect cellular activity. This thesis is concerned with the effects of ANI on both passive and active membrane properties of single cells recorded intracellularly in order to determine how ANI may function to eliminate neural activity.

Memory

Memory can be defined as the retention and recall of past experience. Declarative memory in particular involves the conscious recollection of facts and events (Cohen and Squire, 1980; Squire et al., 2004). Procedural memories, on the other hand, are a type of implicit memory that are exhibited through performance rather than recollection (Squire et al., 2004). The distinction between conscious and subconscious recollection has been extensively studied

beginning in the 1950's. This started with the investigation of a patient who received bilateral medial temporal lobe resection, for the treatment of intractable seizures (Scoville and Milner, 1957). The importance of the hippocampus (a medial temporal lobe structure) was popularized with the study of one such patient, referred to as H.M., who was unable to form new memories of facts and events following removal of a large portion of his temporal lobes. It is now well known that declarative memories are dependent on the medial temporal lobe, and the hippocampus in particular (Squire et al., 2004).

The empirical study of memory processes began with Herman Ebbinghaus' introduction of the concept of "retroactive interference." This is the idea that recently formed memories could be disrupted through the presentation of new information, and laid the groundwork for the idea of consolidation (Ebbinghaus 1885 as cited by (Hernandez and Abel, 2008; Moser et al., 2015). The process of consolidation was then first hypothesized at the end of the 19th century by Georg Elias Muller and Alfons Pilzecker (Muller and Pulzecker, 1900 as cited by (Lechner et al., 1999; McGaugh, 2000). The term consolidation is derived from Latin, meaning "to make firm" and is a time dependent process over which memories are thought to become permanently stable.

According to consolidation theory, memories move through distinct stages. Working memory lasts for seconds to minutes and corresponds to online information processing (Stern and Alberini, 2013). This is followed by short-term memory (STM), in which information is held offline for a short period of time (minutes to hours). Consolidation is hypothesized to be the process that allows the transformation of labile short-term memories into a more permanent state. Retrieval is then the process of recovering these long-term memories, during which they are thought to return to a labile state in order to be reconsolidated (Stern and Alberini, 2013). Figure 1 illustrates the relationship between the strength of short- and long-term memories over time.

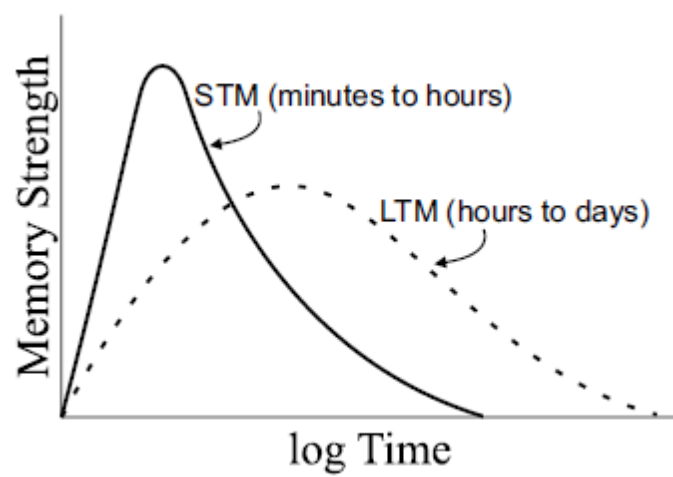
These two stages of memory appear to be independent parallel processes, as each can be interfered with selectively (McGaugh, 2000). One such example is the observation is that post-learning PSI administration seems to selectively inhibit long-term memory (LTM), while leaving STM intact. Furthermore, similar administration of stimulant drugs has been shown to enhance memory (for review see (McGaugh, 1966). While it is acknowledged that neural activity is important, it is argued that the common final pathway is protein synthesis dependent because PSIs can block the formation of memory. The overlooked aspect of this theory is the possibility that neural activity is itself dependent on protein synthesis.

Protein Synthesis Inhibitors and Memory

The *de novo* protein synthesis hypothesis postulates that the translation of new proteins is required for the formation of new memories (Davis and Squire, 1984). In these studies acquisition training (i.e., learning) appears normal and short-term memory is intact, while retention is impaired when long-term memory is tested (Flexner and Flexner, 1967; Barondes and Cohen, 1968; Flexner and Flexner, 1970; Flexner et al., 1973; Flexner and Goodman, 1975; Flood et al., 1975; Davis et al., 1976). Several different memory tasks were tested in these early studies including maze learning (Flexner et al., 1963; Flexner and Flexner, 1967, 1970), active shock avoidance (Barondes and Cohen, 1966, 1968; Flood et al., 1975), visual discrimination (Squire and Barondes, 1972), and object-discrimination (Squire and Barondes, 1973).

Results on memory have also been relatively consistent using various PSIs (such as puromycin, cycloheximide, anisomycin and emetine), all of which inhibit translation, albeit through different mechanisms. Puromycin, one of the first popular PSIs used in the study of

Figure 1: Stages of Memory. Memory can be divided into two time-dependent stages that are differentially affected by modulation. While short-term memory is stronger, it decays fast. Long-term memory takes a longer time to stabilize, but once it does can last for years. Adapted from (McGaugh, 2000).



memory, blocks translation by causing premature release of the growing polypeptide chain (Pestka, 1971). This results in a buildup of peptidyl-puromycin molecules that may contribute partly to its effects on memory (Gambetti et al., 1968). Cycloheximide, a glutaramide antibiotic, interferes with the translocation step in protein synthesis, thereby blocking translational elongation (Obrig et al., 1971). Anisomycin inhibits the peptidyl transferase reaction before polypeptides are released from the polyribosome (Grollman, 1967). Lastly, emetine exerts its effects on protein synthesis through inhibition of the aminoacyl-sRNA transfer reaction, which results in the incorporation of the aminoacyl into a polypeptide-bound form (Grollman, 1966).

Issues with the de novo hypothesis

There are many findings that question the *de novo* protein synthesis hypothesis of long-term memory formation and maintenance. First of all at the behavioural level, many studies have shown the recovery of memories, either spontaneously or evoked, in a variety of conditions following treatment with PSIs (Flexner and Flexner, 1967, 1970; Squire and Barondes, 1972; Flexner and Goodman, 1975; Lattal and Abel, 2004; Ryan et al., 2015). In addition, altering the state of arousal following training under cerebral protein synthesis inhibition can lead to memory recovery. Various stimulants working on the adrenergic system have been shown to reverse the effects of PSIs on memory when administered after training (Barondes and Cohen, 1968; Roberts et al., 1970; Serota et al., 1972). Administration of a foot shock, as well as corticosteroid injections, have also been shown to aid in memory recovery in similar conditions (Barondes and Cohen, 1968). Despite the administration of PSIs, it has been repeatedly shown that memories can be recovered.

The recovery of memories lost following the application of PSIs is not limited to stimulants. Memory lost due to the application of puromycin was recovered following saline injections at various time points ranging from 4-10 hours to 30-60 days (Flexner and Flexner, 1967). The same group showed later that injections of various salt solutions as well as ultra-filtered blood serum and distilled water could seemingly restore these memories four days later (Flexner and Flexner, 1970). As mentioned earlier, the effects of puromycin are likely exaggerated by the accumulation of toxic peptidyl-puromycin products, which would be diluted following these various injections. The problem here, however, is that if puromycin was indeed blocking consolidation, recovery of the memory should not be possible under any condition.

In a study using cycloheximide, which does not create potentially toxic by-products like puromycin, spontaneous recovery of memory occurred after three days, even though total amnesia was observed three hours after training (Squire and Barondes, 1972). Similar results have been observed using anisomycin (a similarly 'safe' PSI) in a contextual fear conditioning paradigm (Lattal and Abel, 2004). This study investigated the effects of protein synthesis inhibition on reconsolidation of the memory trace, the process by which reactivation of a consolidated memory brings it back into a labile state. These authors found that if anisomycin was administered following memory acquisition, the animals appeared amnesic one and 21 days later. If the drug was administered following normal retrieval, however, amnesia was observed one day later, but the memory was intact 21 days later (Lattal and Abel, 2004). Based on these results, it appears as though the initial memory impairment was not due to disruption in reconsolidation of the original memory trace. If reconsolidation was, indeed completely blocked by protein synthesis inhibition, recovery of the memory should not occur.

Protein synthesis inhibitors have also been shown to cause large changes in neurotransmitter release. A variety of early experiments showed decreased activity of tyrosine hydroxylase (an enzyme necessary for synthesis of catecholamine neurotransmitters) following PSI administration (Flexner et al., 1973; Flexner and Goodman, 1975). More recent work has shown large increases in biogenic amines in both the hippocampus and amygdala when they are the respective targets for protein synthesis inhibition (Canal et al., 2007; Qi and Gold, 2009). In the amygdala, this surge of neurotransmitter release is followed by a subsequent severe reduction in the amount of biogenic amines present. More convincingly, β -receptor agonists and antagonists administered in order to dampen these surges and depletions in transmitter release have been shown to attenuate anisomycin-induced amnesia (Canal et al., 2007).

Influence of PSIs on neural activity

Many early studies found detrimental effects of puromycin on neural activity. One such study showed that puromycin, but not cycloheximide, completely abolished hippocampal activity recorded 5 hours after injection (Cohen et al., 1966). Similar results were obtained when testing the effects of protein synthesis inhibition on vagal nerve activity (Dahl, 1969). In this case puromycin, but not cycloheximide or chloramphenicol (a mitochondrial protein synthesis inhibitor), decreased the height of the nerve spike potential and diminished the positive after-potential as well as the post-tetanic hyperpolarization. Puromycin has also been shown to induce seizure activity in the hippocampus as well as lower the threshold for seizures elicited by a normally sub-convulsive dose of pentylenetetrazol (Cohen and Barondes, 1967).

Because of the issues with puromycin, seemingly above and beyond its inhibition of protein synthesis, it has been since abandoned in favour of other PSIs with seemingly less

detrimental neurobiological and behavioural effects (such as cycloheximide and ANI). These drugs are not, however, without their own problems. Electroencephalogram (EEG) recordings following cycloheximide administration showed a decrease in the duration and occurrence of slow wave activity and a decrease in the occurrence of small high frequency bursts (Luttges et al., 1972; Wilcox et al., 1974). Power spectra of EEG recordings also showed dose-dependent changes in the dominant frequencies following cycloheximide treatment. Increases in cycloheximide dose resulted in proportionately lower frequency activity (Wilcox et al., 1974).

It has been suggested that PSIs such as ANI have better relative specificity and a lower prevalence of physical and behavioural effects that could confound observed memory deficits. However, ANI, despite this conjecture, has been shown to affect a wide variety of processes. Although many neurophysiological properties of neurons in the abdominal ganglion of *Aplysia* were found to be unaltered following the application of anisomycin, the pacemaker activity of spontaneously active neurons was affected, as was the spike frequency, which decreased over time in a manner correlated with decreased amino acid incorporation (Schwartz et al., 1971). Another study showed that anisomycin administration resulted in the abolishment of cortical evoked potentials as well as the disruption of the functional representation of the motor map following ANI administration (Kleim et al., 2003). The authors interpreted this information as evidence that motor map representation is protein synthesis dependent. One could argue, however, that this disruption may have been due to the inhibition of neural activity as similar issues were observed following sodium channel blockade. More recent work from our lab has shown that ANI indeed causes a dramatic reduction in both spontaneous and evoked local field potential (LFP) recordings, correlated to the actual level of protein synthesis inhibition (Sharma et al., 2012). This inhibition of neural activity was further investigated using various assays of

online behaviour. Injections of ANI into the ventral, but not the dorsal hippocampus had anxiolytic effects on both an innate and trained test of anxiety, to a similar degree as agents known to directly inhibit neural activity (Greenberg et al., 2014). These online effects were also studied using a version of the Morris Water Maze task that is known to require the dorsal hippocampus. Rats with an inactivated dorsal hippocampus, either by ANI or the sodium channel blocker tetrodotoxin (TTX), were unable to perform the allocentric navigation version of the task, while performing as well as control animals in visually-cued navigation (Dubue et al., 2015).

Elucidation of a Protein Synthesis Dependent Depression of Neural Activity

As discussed, there is ample evidence to suggest that PSIs interfere with neural activity (Kleim et al., 2003; Sharma et al., 2012; Greenberg et al., 2014; Dubue et al., 2015). However, to date, there have been no studies that have both applied ANI and investigated basic cellular responses with intracellular recordings. In this thesis, the goal is to investigate how this is manifested at a cellular level, as well as the mechanism through which this might be occurring. Because of the aforementioned involvement of the hippocampus in declarative memory, I will be recording from specialized cells within the hippocampus.

Hippocampal anatomy

The hippocampus, whose namesake comes from its apparent resemblance to a seahorse (Lewis, 1923), is a limbic cortical structure located in the medial temporal lobe. The hippocampal area can be divided into the dentate gyrus (DG) and cornu Ammonis (CA; “Ammon’s Horn”) 1, 2, and 3 (CA1, CA2, and CA3; Figure 2; (Andersen et al., 1969). Information flow in the hippocampus is thought to occur through the trisynaptic pathway. As

shown in Figure 3, information comes into the hippocampus through the perforant path (PP) from the entorhinal cortex (EC), to the dentate gyrus, through the mossy fibre (MF) pathway from the dentate to CA3, and lastly through the Schaffer collaterals of pyramidal cells in CA3 to CA1 (SC/AC). According to the lamellar hypothesis, transfer of information through this trisynaptic pathway occurs within many lamella, organized in the same transverse plane (Andersen et al., 1969). Information in the hippocampus also flows along the longitudinal axis, both ipsilaterally and from CA3 to the contralateral CA1 through the hippocampal commissures.

CA1

As mentioned above, area CA1 receives input from CA3 via the Schaffer collaterals. Projections are also received from CA3 of the contralateral hemisphere via commissural fibres (Amaral and Witter, 1989). CA1 pyramidal neurons also receive innervation from layer III of the EC (Witter et al., 1988), the nucleus reuniens of the thalamus (Krettek and Price, 1977; Wouterlood et al., 1990), and the basolateral nucleus of the amygdala (Kemppainen et al., 2002). Projections from layer III of the EC are topographical in nature, with fibres from the lateral entorhinal cortex (LEC) projecting to the distal area of CA1, and those from the medial entorhinal cortex (MEC) terminating in the proximal area of CA1 (Witter et al., 1988). Output from CA1 also forms the principal hippocampal-cortical projection, from CA1 back to the EC via the subiculum (Witter et al., 2000).

Because of their importance in hippocampal circuitry, as well as their viability in acute slice preparations, CA1 pyramidal neurons are a very well characterized cell type. As shown in Figure 3, these neurons have cell bodies located in stratum pyramidale, an apical dendritic tree located in stratum radiatum, extending into stratum lacunosum moleculare, and a proximal

dendritic tree located in stratum oriens (Pyapali et al., 1998). Input from CA3 (via the Schaffer collaterals) projects onto CA1 neurons at the level of stratum radiatum and stratum oriens, while projections from EC layer III innervate at the level of stratum laculosum moleculare (Pyapali et al., 1998).

Pyramidal neurons located in the CA1 region of the hippocampus form the major output of the hippocampus and collect the result of hippocampal processing to send to the subiculum and EC (Dvorak-Carbone and Schuman, 1999). Axons from CA1 pyramidal neurons send minimal intrahippocampal projections, the most significant being topographically organized projections to the subiculum, a major hippocampal output (Tamamaki et al., 1987).

Extrahippocampal CA1 projections leave via the fimbria, and project to different areas depending on their location along the septo-temporal axis. Neurons in the septal region project to the retrosplenial and perirhinal cortices, the lateral septal nucleus, and the diagonal band of Broca. Neurons in the midsepto-temporal region project to the taenia tecta and the medial frontal cortex. Lastly, neurons in the temporal region send projections to the anterior olfactory nucleus, the olfactory bulb, the nucleus accumbens, the basal nucleus of the amygdala, and the anterior/dorsomedial hypothalamus (see Figure 3; (Jay et al., 1989; van Groen and Wyss, 1990).

Figure 2: The Hippocampal Formation. Shows the hippocampal formation in the rat brain running rostrally from the septal nuclei (S) to the temporal cortex (T) in the shape of a “C.” The hippocampal slice is perpendicular to the septo-temporal axis, in the transverse plane. Information flows through the trisynaptic pathway starting with the perforant path (PP) from the entorhinal cortex (EC) to the dentate gyrus (DG), from the DG along the mossy fibre (mf) pathway to CA3, and from CA3 to CA1 via the Schaffer collaterals (sc). CA1 neurons also send axons to the subiculum (S), which completes the loop by sending axons back to the EC. From (Amaral and Witter, 1989).

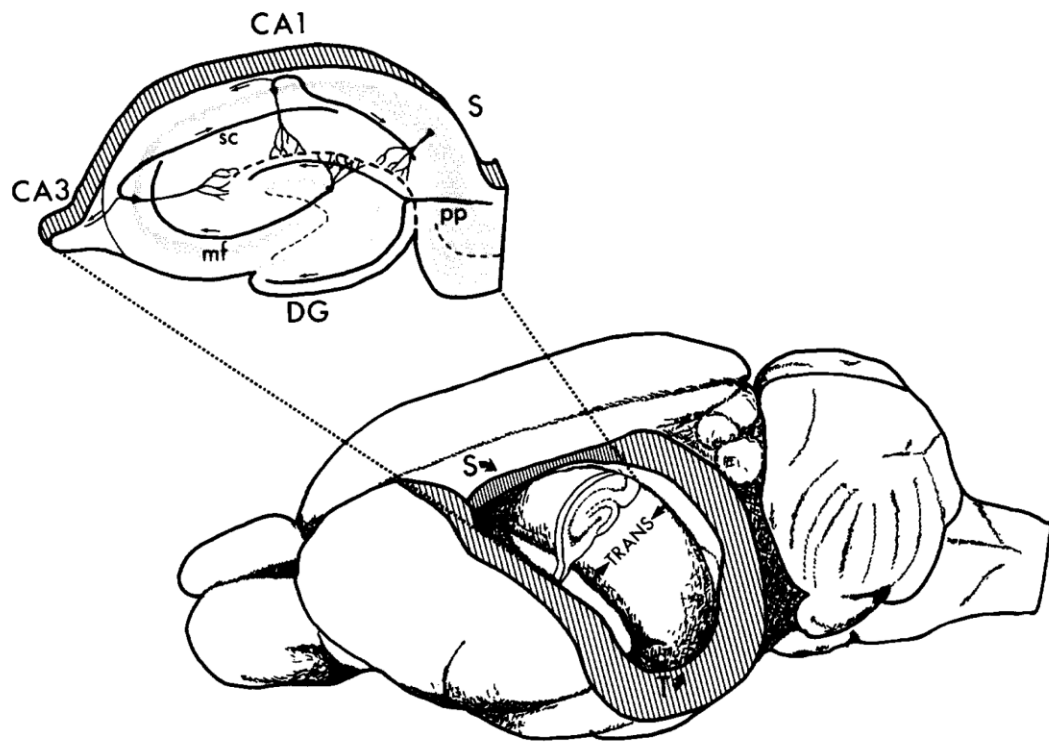


Figure 3. Neural Connectivity in the Hippocampus. Information flows unidirectional through the hippocampus. Entorhinal input travels from the entorhinal cortex (EC) through the perforant path (PP) to the dentate gyrus (DG) via the medial perforant path (MPP) which innervates the medial DG molecular layer, and the lateral perforant path (LPP) which innervates the outer molecular layer of the DG. Dentate granule cells then send projections via the mossy fibre pathway (MF) to area CA3. Pyramidal neurons in CA3 in turn send axons along the Schaffer Collateral pathway (SC) back to the EC, as well as to contralateral CA1 via the associational commissural pathway (AC). Pyramidal neurons in CA1 also receive direct input from the PP, as well as send axons to the subiculum (Sb). Neurons in the Sb complete the loop by sending hippocampal output back to the EC. Image from <http://www.bristol.ac.uk/synaptic/pathways/>

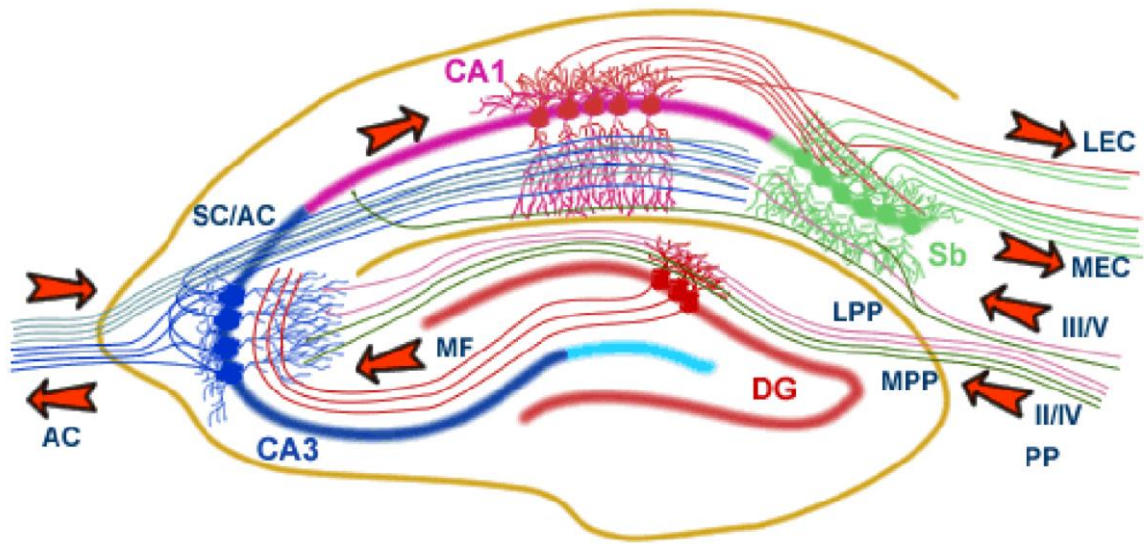
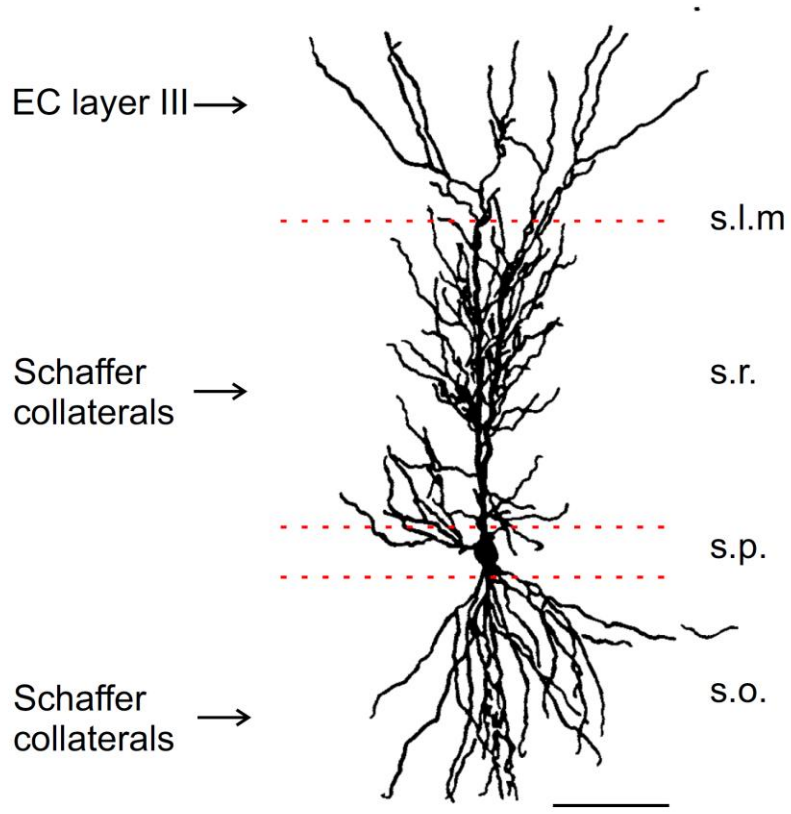


Figure 4: CA1 Pyramidal Cell Morphology and Synaptic Inputs. Shows an adult rat CA1 pyramidal neuron (camera lucida drawing). The cell body is located in the pyramidal cell layer (stratum pyramidale; s.p.), basal dendrites in stratum oriens (s.o.), and apical dendrites in the stratum radiatum (s.r.), extending into the stratum lacunosum moleculare (s.l.m.). Major excitatory inputs for each layer are also shown. The Schaffer collaterals synapse at the level of s.r. and s.o., while EC layer III inputs synapse at the level of s.l.m. Scale bar = 100 μ m. Adapted from (McGaugh, 1966; Bannister and Larkman, 1995).



Purpose

The overall aim of this thesis was to investigate the effect of the protein synthesis inhibitor anisomycin on both passive and active neuronal membrane properties of pyramidal cells of the hippocampal CA1 region. Considering the extensive documentation of the cellular properties of CA1 neurons, as well as their integral role in hippocampal processing, these pyramidal cells are an excellent model for exploring the single-cell and membrane effects of anisomycin administration. Given the effects observed of anisomycin at both the behavioural and neural population level, it is important to understand how individual neurons are affected, as well as why these changes might be occurring.

Materials and Methods

Preparations and Solutions

Experiments were performed on transverse hippocampal slices from male Sprague Dawley rats weighing 50-100 g (approximately 3-4 weeks old). All procedures were performed in accordance with Canadian Council of Animal Care guidelines, and protocols (#092) were approved locally by the Biosciences Animal Care and Use Committee at the University of Alberta. Rats were anesthetized in a gas chamber containing 4% isoflurane in 100% O₂ (Benson Medical Industry Inc, Markham, ON). Following loss of the righting reflex, rats were decapitated, and their brains were placed into an ice cold (0-4°C) slicing solution containing (in mM): 124 NaCl, 3 KCl, 1.4 NaH₂PO₄, 1.3 MgSO₄, 26 NaHCO₃, 1.5 CaCl₂, 10 glucose (Fisher Scientific, Toronto, Ontario, Canada), and saturated with carbogen (5% CO₂/95% O₂; Praxair Canada Inc., Mississauga, Ontario). All extracellular solutions had an osmolarity of 303 ± 3 mOsm. Transverse hippocampal slices were cut at a thickness of 300 µm using a Leica VT1000 S vibrating blade microtome (Leica, Bannockburn, IL) and placed in room temperature artificial cerebral spinal fluid (aCSF) solution containing (in mM): 124 NaCl, 3 KCl, 1.4 NaH₂PO₄, 1.3 MgSO₄, 26 NaHCO₃, 1.5 CaCl₂, 10 glucose, and saturated with carbogen. Slices were allowed to recover in carbogenated aCSF at room temperature for one hour before any recordings were made. ANI (Sigma Aldrich) was dissolved in hydrochloric acid and brought to volume with phosphate buffered saline in order to reach a final concentration of 100 mM.

Electrophysiology

Slices were transferred to a fixed stage of an upright microscope (Leica DM-LFS) that was perfused with a continuous flow (2-4 mL/min) of aCSF maintained at 34.0 ± 1.0 °C (Bipolar Temperature Controller, Warner Instruments, Hamden, CT) via A Miniplus 3 peristaltic

pump (Mandel Scientific, Guelph, ON). CA1 pyramidal neurons were visually identified using a 40X water-immersion objective and infrared differential interference contrast imaging and a near-infrared charge-coupled device camera (Sony XC-75). Whole-cell patch clamp recordings were obtained using borosilicate glass pipettes (2-6 M Ω) pulled using a Flammig/Brown micropipette puller (Model P97, Shutter Instrument Company, San Francisco, CA) and filled with intracellular solution containing (in mM): 135 K-Glu, 10 HEPES, 10 EGTA, 7 KCl, 2 MgCl₂, 0.3 Na₂GTP, 3 MgATP, 10 phosphocreatine (Sigma Aldrich, St, Louis, MO), pH 7.2-7.3, 290-295 mOsm. Recordings were made using an Axon Multiclamp 700B amplifier (Axon Instruments/Molecular Devices, Sunnyvale, CA) and digitized at a sampling rate of either 20 (continuous membrane voltage), 50 (current sweep and ramp protocols), or 250 kHz (single spike protocols) using an Axon Digidata 1322A driven by pClamp software (Axon Instruments/Molecular Devices). The pipette offset was measured following the conclusion of the experiment by physical patch breakout and was corrected for individual experiments. The liquid-liquid junction potential was empirically determined to be -7 mV using the method of Neher (Neher, 1992) but was not corrected.

Whole-cell patch-clamp recordings were made in visually identified CA1 pyramidal neurons, and were allowed to stabilize for more than four to five minutes before the beginning of baseline recordings. In every case, baseline measures of resting membrane potential and single spike thresholds were acquired. In some cases, a family of hyperpolarizing and depolarizing current pulses (in 50 pA steps) as well as current ramps were applied to also investigate baseline active membrane properties. The maximum deflection of the ramps were increased in 50 pA steps, increased linearly from 0 pA (i.e, 0 to 50 pA, 0 to 100 pA, 0 to 150 pA, and so on), and were one second in duration. Following this baseline recording period, these measurements were

repeated at seven minute intervals following perfusion with either the same control aCSF solution or one which contained 100 μ M ANI. In every case in which membrane properties were assessed with current pulses or ramps, the resting membrane potential was equalized to baseline levels using current injections. In the case of ANI perfusions, after 21 minutes, the perfusion medium was switched back to normal aCSF before the last acquisition period at 28 minutes.

In order to assess input resistance and the membrane time constant, low intensity (-10 pA) short (500 ms) hyperpolarizing pulses were applied every minute during continuous recordings. In the cases in which membrane potential fluctuated from baseline measures, current was used to correct it to the same level. Input resistance was calculated by measuring the steady-state deflection in voltage (ΔV) as a function of the amount of current (I) applied ($R_{\text{input}}=V/I$). The same hyperpolarizing pulses were used to calculate the membrane time constant ($\tau=R_m C_m$) by fitting a single order exponential curve ($f(t) = A_i e^{-\frac{t}{\tau_i}} + C$) to the membrane deflection.

Single spike characteristics were assessed by applying short (3.2 ms) depolarizing pulses in order to elicit a single action potential (AP), while multiple spike characteristics were assessed using longer (1 second) depolarizing pulses. The threshold of the first AP was calculated using Matlab (The Mathworks, Natick, MA) and was defined as the point at which the differential of the voltage (V_m) as a function of time exceeded double the value of baseline fluctuations for seven consecutive data points, indicating the presence of an AP. We confirmed visually that this method successfully demarked spike threshold. Spike amplitude was measured as the difference in voltage between the threshold and the peak amplitude of the spike. Spike duration at half-amplitude (half-width) was defined as the width of the spike at the half-point between threshold and the peak.

Multiple spike characteristics were assessed using long (1 second) current sweeps. The medium after-hyperpolarization was measured as the voltage deflection from baseline following the termination of these depolarizing current sweep for which multiple spikes were elicited. The frequency of AP firing in long depolarizing pulses was calculated by counting the number of action potentials elicited and dividing by the duration of the pulse. This was done at three intensity levels, which varied between cells.

Autoradiography

The degree of protein synthesis inhibition was evaluated *in vitro* following bath incubation experiments using ANI. Slices were prepared identically to those in the electrophysiological experiments, and were incubated in control aCSF or ANI solution (100 μ M ANI in aCSF). Following a 30 minute incubation, slices were transferred to a solution with 10 mCi/mL 35 S cysteine/methionine in aCSF for 30 minutes, and then dried overnight. Dried slices were placed under Kodak BioMax MR X-Ray film (PerkinElmer, Waltham, Massachusetts) for 7-8 days. Control and ANI slices from the same experiments were always developed on the same film to ensure identical exposure times. Once developed, grayscale digital images were scanned at a resolution of 2400 DPI (HP ScanJet G3110, Hewlett-Packard Company, Palo Alto, CA) and analyzed using ImageJ (National Institutes of Health, Bethesda, Maryland). Light intensity values (from a standard scale ranging from 0 to 255, with 255 being the brightest and 0 being the darkest) were averaged across the entire slice following selection of the region of interest by hand, omitting any spaces. In relation to this study, less amino acid incorporation, and therefore less protein synthesis, was indicated by a higher value on this scale. These raw values were then normalized to the background (lightest area on the page) and the darkest slice, resulting in a higher normalized value representing darker imaging, and therefore more protein synthesis.

Triphenyltetrazolium chlorides staining

The effects of ANI on mitochondrial activity were assessed using 2,3,5-triphenyltetrazolium chloride (TTC; Sigma Aldrich), an indicator of cellular respiration (Riepe et al., 1996). The conversion of white TTC to 1,3,5-triphenylformazan, which is red in colour, provides a measure of the amount of electron transport occurring at the time of application of TTC to the tissue (Riepe et al., 1996). Slices were incubated in either control aCSF or 100 μ M ANI before being transferred to a 2% TTC solution in aCSF for 30 minutes. Slices were then transferred to a 4% buffered formalin solution overnight before being mounted on hanging drop slides (Fisher Scientific). Slices were scanned in grayscale and analyzed using ImageJ, and were quantified via light intensity values, as with autoradiography experiments, although images were scanned at 4800 DPI.

Statistical analysis

Statistical analysis on electrophysiological data was performed using a repeated measures one-way analysis of variance (ANOVA) on control and ANI data across all time points. *Post hoc* Tukey HSD tests were used to look for significant changes ($\alpha = 0.05$) between baseline values and each time point when a main effect was observed.

A Student's t-test was used to assess differences between normalized light intensity values of control and ANI slices in autoradiography and TTC experiments.

Results

Bath application of ANI inhibits protein synthesis in hippocampal slices

To confirm that a short (20-30 minute) application of a low concentration (100 μ M) of ANI could inhibit protein synthesis in transverse hippocampal slices, we measured, using autoradiography, the incorporation of 35 S cysteine/methionine. Average light intensity values of individual slices ($n = 4-6$ for each group, 4 experiments total, $n = 4$) were quantified using ImageJ and were normalized (from 0 to 1) to the minimum and maximum values for each experimental scan batch that included both ANI and control treatment conditions. Following this normalization, a value of 1 represented the darkest intensity value (i.e., the maximal autoradiographic signal) while 0 represented the background level of intensity. As seen in Figure 5, ANI treated slices (0.48 ± 0.05) exhibited significantly less protein synthesis than control slices (0.86 ± 0.02), confirming that a 30 minute bath application of 100 μ M ANI inhibits protein synthesis in acute hippocampal slices ($P < 0.01$). This corresponds to a 55.8 % decrease in protein synthesis following ANI treatment.

ANI cause a loss of membrane potential without changing other passive membrane properties in CA1 neurons

To investigate the effect of ANI on membrane properties, we targeted CA1 pyramidal neurons for whole-cell patch-clamp recordings in transverse hippocampal slices. The resting membrane potential (RMP) was reported as the voltage recorded when no holding current was applied (Control, $n = 16$; ANI, $n = 29$). Figure 6A and 6B show example traces from a control

Figure 5: Anisomycin inhibits protein synthesis in hippocampal slices.

Normalized light intensity data from autoradiographs of ^{35}S amino-acid incorporation experiments. Scatter plots show average data (\pm SEM), while the lines show within-experiment averages (\pm SEM). There was a significant decrease (from 0.67 ± 0.09 to 0.49 ± 0.08 , $P < 0.01$) in the normalized amount of incorporated ^{35}S labelled cysteine and methionine in slices treated with $100 \mu\text{M}$ ANI for 30 minutes, as compared to controls. Insets show example autoradiographs from each group. Darker staining and a higher normalized intensity equate to more amino acid incorporation and therefore a greater level of protein synthesis. Inset shows four example transverse hippocampal slices used in each of the control and ANI conditions. Scale bar corresponds to 4 mm.

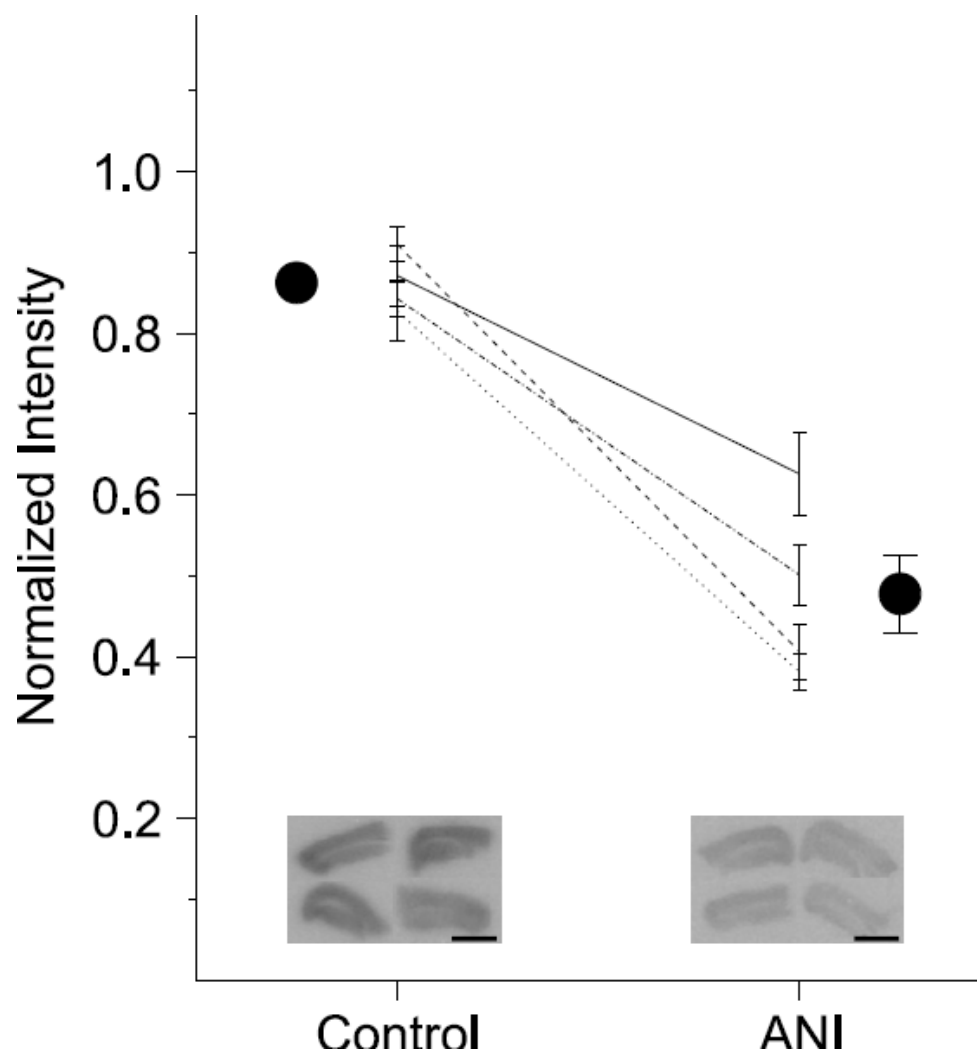
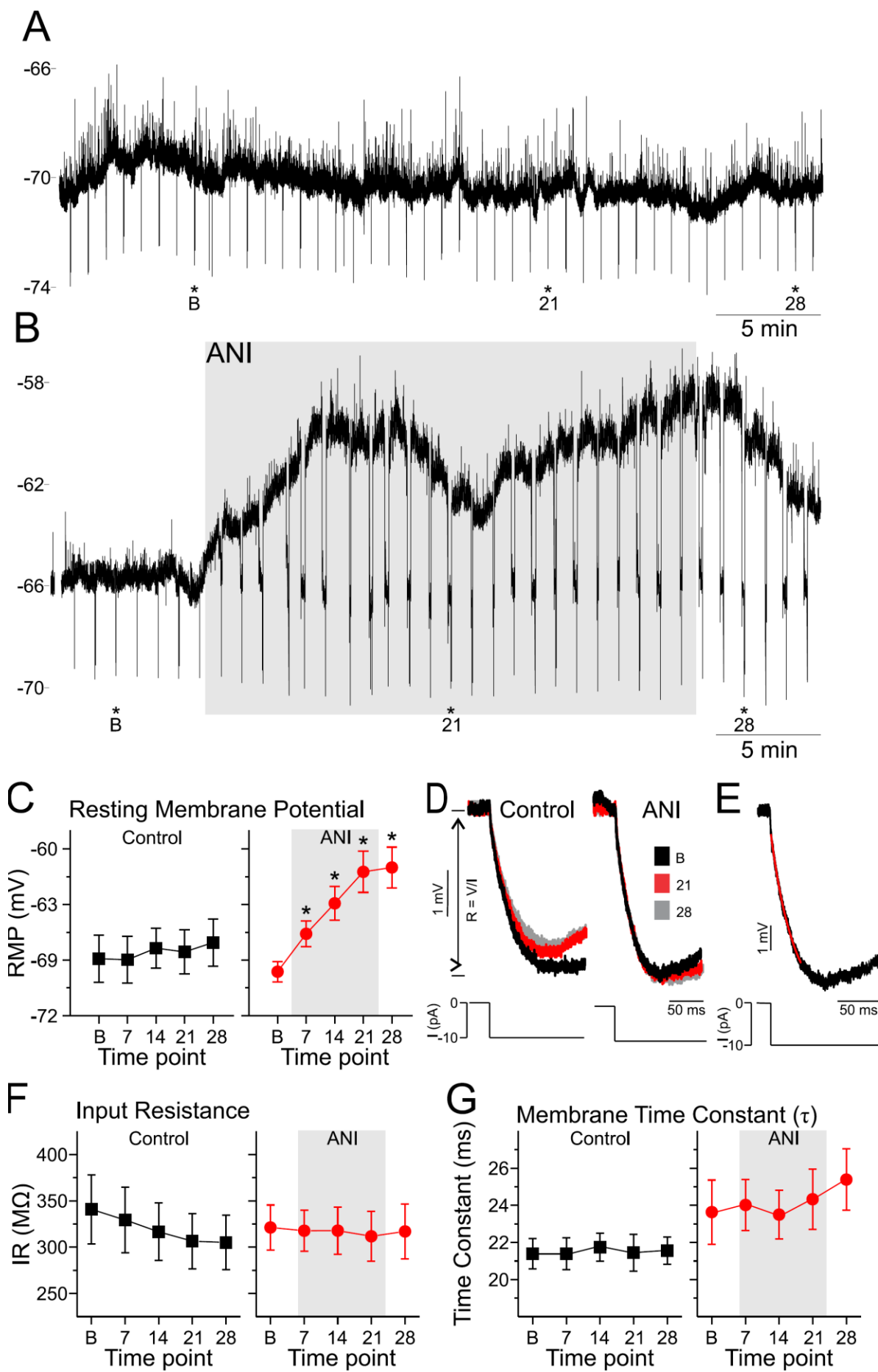


Figure 6: Anisomycin significantly depolarizes CA1 cells, but does not change input resistance nor membrane time constant. **A.** Sample trace of a raw continuous whole-cell patch-clamp recording from a control cell showing a relatively steady RMP throughout the duration of the recording. **B.** Sample trace of a similar recording from an ANI treated cell showing a depolarization of the RMP following 100 μM bath application of ANI (shaded area). Small (-10 pA) hyperpolarizing pulses were given every 60 seconds in order to track input resistance and tau over time. Inset shows example traces from baseline (black), during ANI application (red), and the post-ANI period (gray). Asterisks denote where in the sample trace the inset traces were taken from. **C.** Average resting membrane potential in control (black squares, left) and ANI treated cells (red circles, right) as a function of time following manipulation (baseline, B; 0-7 minutes of ANI exposure, 7; 7-14 minutes of ANI exposure, 14; 14-21 minutes of ANI exposure, 21; post-ANI exposure, P). While there are no changes in control cells, there is a significant depolarization of the RMP in ANI treated cells at all time points following bath application (shaded area) as well as into the post-ANI period. **D.** Shows average input resistance during the same time points as in A (control) and B (ANI) for control (left) and ANI (right) cells. **E.** Raw trace showing a single order exponential decay function (red) fit to the responding trace to a 10 pA hyperpolarizing pulse. **F.** There are no significant changes in input resistance in control (black squares, left), nor ANI treated cells (red circles, right) at any time point. **G.** Shows the average membrane time constant in control (black squares, left) and ANI (red circles, right) treated cells at the same time points as above.



and ANI cell, respectively. The noise observed in these traces likely corresponds to spontaneous synaptic activity. It is unlikely that this presynaptic activity is affected by translational inhibition. RMP was extracted from spontaneous recordings during baseline conditions (0-7 minutes: base), at three time points spaced at seven minute intervals following addition of ANI to the perfusate (7, 14, and 21 minutes), as well as 7 minutes following restoration of control aCSF, or 28 minutes following ANI application. In control cells, measurements were taken at the same time points, however, no ANI was added to the perfusate. In cells where active membrane properties were assessed, the RMP for seven minutes of continuous data was averaged. In cells where passive membrane properties were assessed, I averaged the membrane potential over a seven minute period in which no changes in current were delivered. In cells where passive membrane properties were analyzed, we averaged the membrane potential over seven separate one minute segments in which no changes in current were delivered. As expected, and as illustrated in Figure 6A-B, control cells showed stable RMP values across this entire period. During all applications of ANI, however, RMP values depolarized by 5-10 mV after 21 minutes of perfusion. On average, these changes were significant as demonstrated by a one-way repeated measures ANOVA ($F(4,112) = 23.02, P < 0.0001$). Tukey HSD *post hoc* tests revealed that the average resting membrane potential depolarized from -70 ± 1 mV at baseline to -68 ± 1 mV 7 minutes post ANI, ($P < 0.05$), -66 ± 1 mV 14 minutes post ANI, ($P < 0.01$), -63 ± 1 mV 21 minutes post ANI ($P < 0.01$), and was maintained at -63 ± 1 mV seven minutes following reperfusion with regular aCSF ($P < 0.01$). In contrast, there were no significant changes over time in control cells at identical recording times ($F(4,60) = 1.03, P > 0.05$). Average resting membrane potential responses for control (black squares) and ANI (red circles) data is summarized in Figure 6E.

In a subset of experiments designed for investigating other passive membrane properties, small (-10 pA) hyperpolarizing pulses (500 ms) were administered every minute in both control (Figure 6A, C) and ANI (Figure 6B, C) conditions. In these protocols, holding current was applied if necessary to bring the cell back down to the baseline RMP ten seconds before the application of the pulse in order to compensate for any changes in RMP that could affect the values obtained for input resistance and the membrane time constant, τ . Care was also taken to insure the bridge was balanced during these manipulations using the built in bridge balance function and visual conformation using pClamp software (Axon Instruments). Input resistance was calculated by measuring the maximal voltage deflection (ΔV) as a function of the amount of current (I) applied ($IR = \Delta V/I$). There were no significant changes in input resistance in either control ($n = 7$, $F(4,24) = 0.19$, $P > 0.05$) or ANI ($n = 12$, $F(4,40) = 0.43$, $P > 0.05$) cells. Figure 6E shows average control (black squares) and ANI (red circles) data. Figure 6C shows examples of the responding voltage deflections before (black), during (red), and after (gray) ANI application (right), as well as at the corresponding time points in control cells (left). The membrane time constant (τ) was calculated by fitting a single order exponential ($f(t) = A_i e^{-\frac{t}{\tau_i}} + C$) to the membrane deflection. Figure 6D displays an example trace showing the exponential decay fit in red. There were no significant changes in τ in control ($F(4,24) = 0.39$, $P > 0.05$; Figure 6G, black squares), or ANI treated ($F(4,40) = 1.24$, $P > 0.05$; Figure 6G, red circles). These data are summarized in Table 1.

ANI alters single action potential properties of CA1 neurons

Positive current injection was used to elicit a single spike in each neuron across time in order to measure changes in active membrane properties during both control and ANI conditions

Table 1: Passive Membrane Properties. Average resting membrane potential, input resistance, and membrane time constant for control and ANI treated cells. Results of overall ANOVAs are in the left column. If the ANOVA was significant, results of the *post-hoc* Tukey HSD tests, as compared to baseline, are shown below the average.

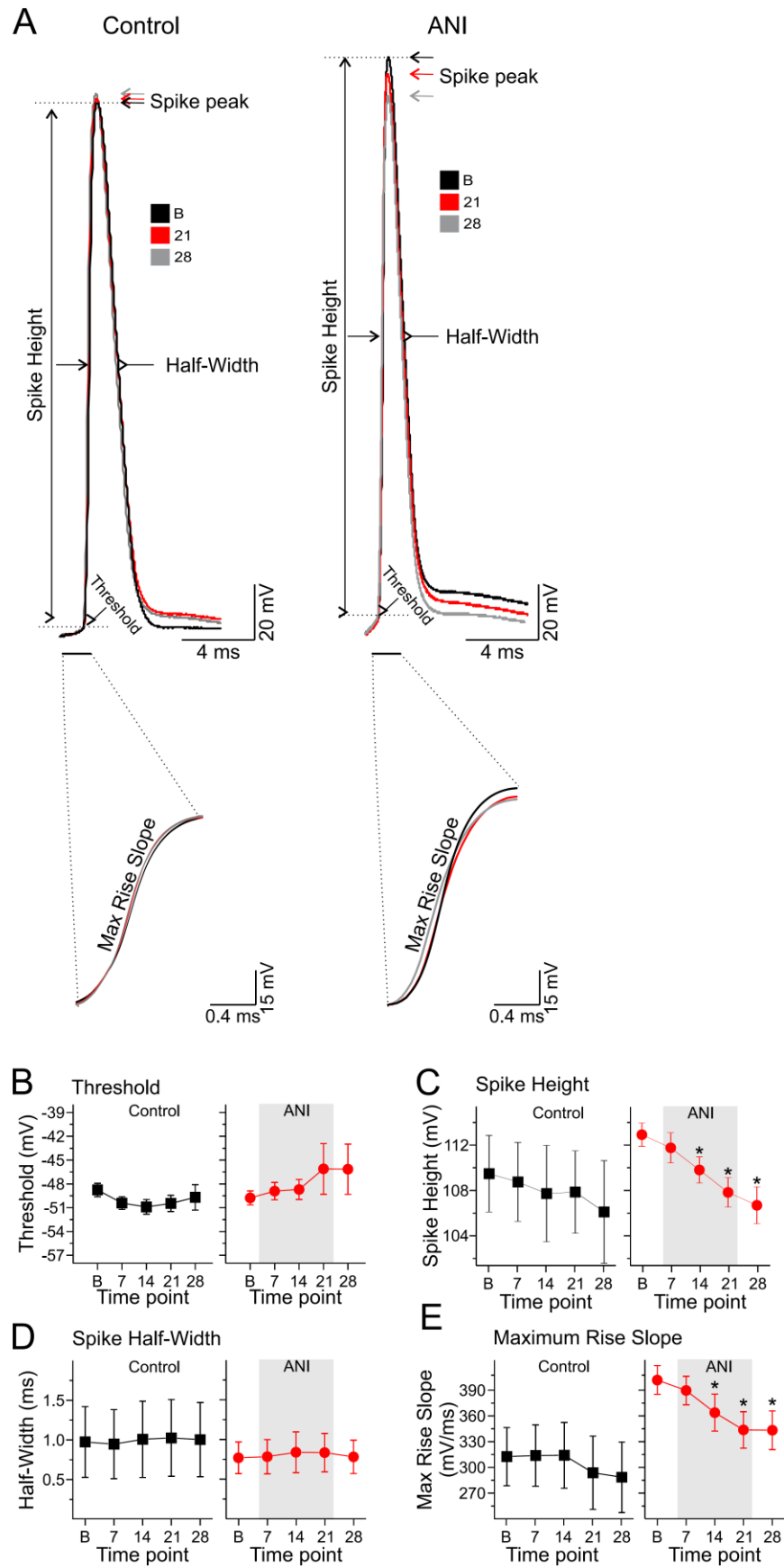
Resting Membrane Potential (mV)					
Control	Baseline	Control-7	Control-14	Control-21	Control-28
$F(4,32)=0.84,$ $P > 0.05$	-69 ± 2	-70 ± 2	-68 ± 1	-69 ± 2	-69 ± 2
ANI	Baseline	ANI-7	ANI-14	ANI-21	ANI-28
$F(4,76)=22.24,$ $P < 0.0001$	-70 ± 1	-68 ± 1 <i>NS</i>	-66 ± 1 $P < 0.01$	-63 ± 1 $P < 0.01$	-63 ± 1 $P < 0.01$
Input Resistance (MΩ)					
Control	Baseline	Control-7	Control-14	Control-21	Control-28
$F(4,24)=0.19,$ $P > 0.05$	$340.75 \pm$ 37.2	329.29 ± 5.5	$316.63 \pm$ 31.1	$306.45 \pm$ 29.7	$305.06 \pm$ 29.3
ANI	Baseline	ANI-7	ANI-14	ANI-21	ANI-28
$F(4,40)=0.23,$ $P > 0.05$	$321.24 \pm$ 24.2	317.7	$317.81 \pm$ 25.5	$311.70 \pm$ 26.3	$316.96 \pm$ 29.5
Membrane Time Constant (ms)					
Control	Baseline	Control-7	Control-14	Control-21	Control-28
$F(4,24)=0.39$ $P > 0.05$	21.39 ± 0.8	21.39 ± 0.9	21.74 ± 0.8	21.44 ± 1.0	21.55 ± 0.7
ANI	Baseline	ANI-7	ANI-14	ANI-21	ANI-28
$F(4,40)=1.24,$ $P > 0.05$	23.63 ± 1.73	24.02 ± 1.4	23.50 ± 1.3	24.33 ± 1.6	25.39 ± 1.7

(see Figure 7A for example traces). Measures of spike threshold, spike peak, spike amplitude, spike half-amplitude duration (half-width), and spike rise and decay slopes were taken at specified time points in both control and ANI perfusion conditions.

Spike thresholds were measured as the voltage at which the initial deflection point of the action potential occurred (Figure 7A). Although there was a trend for a decrease in threshold in control cells (Figure 7B, black squares), and an increase in ANI cells (Figure 7B, red circles), there were no significant changes in either group (control, $F(4,28) = 1.39$, $P > 0.05$; ANI, $F(4,76) = 0.92$, $P > 0.05$). The lack of a change in threshold was confirmed by means of rheobase calculated using current ramps (data not shown).

The spike peak amplitude was defined as the maximum voltage value of the spike, and spike amplitude was measured as the voltage difference between the threshold and spike peak of the first action potential elicited in each group. While there were no changes in control cells ($F(4,28) = 2.61$, $P > 0.05$; Figure 7C, black squares), there was a main effect for a change in spike amplitude in ANI cells ($F(4,76) = 16.48$, $P < 0.0001$; Figure 7C, red circles). The spike amplitude 7 minutes after ANI perfusion (111.76 ± 1.3 mV) was not different than baseline (112.92 ± 1.0 mV, $P > 0.05$), although the decrease was significant 14 (109.81 ± 1.2 mV, $P < 0.01$), 21 (107.83 ± 1.3 mV, $P < 0.01$), and 28 minutes after the addition of ANI (7 minutes after return to regular aCSF; 106.69 ± 1.6 mV, $P < 0.01$). The spike half-amplitude duration (half-width) of the first action potential was measured as the width of the first action potential at half amplitude (halfway between the threshold and spike peak). There were no significant changes in half-width of control ($F(4,28) = 1.45$, $P > 0.05$; Figure 7D, black squares) or ANI cells ($F(4,76) = 1.42$, $P > 0.05$; Figure 7D, red circles).

Figure 7: Effect of ANI on single spike characteristics. **A.** Raw traces showing single spikes during the equivalent of baseline (black), ANI (red), and post-ANI (gray) periods for a control cell (left). Arrows and lines indicate how and where threshold, spike peak, spike amplitude, and half-amplitude duration were measured. Raw traces showing single spikes for similar time points in ANI treated cells (right). **B.** Average data showing no change in threshold in control (black squares, left) or ANI treated cells (red circles, right) from baseline conditions (B), at any time point following ANI application (7, 14, 21, or 28 minutes). **C.** There was a significant decrease in the spike amplitude (measured from threshold to peak) in ANI treated, but not control cells. In ANI cells, the spike amplitude was not different from baseline to 7 minutes following the addition of ANI to the bath solution (7), but was significantly decreased at 14, 21, and 28 minutes following ANI application. **D.** There were no changes in the spike half-amplitude duration in control or ANI treated cells at any time point. **E.** Raw data showing the upward phase of the action potential in order to view the maximum rise slope during baseline (black), ANI (red), and post-ANI (gray) conditions. **F.** There were no significant changes in the maximum rise slope in control cells. In ANI cells, there was no change in the maximum rise slope from baseline at 7 minutes following



The maximum rise slope was measured as the slope of the rising phase of the action potential at its highest value (see raw traces expanded from time bar in Figure 7A). While the overall ANOVA was significant in control cells ($F(4,28) = 3.09, P < 0.05$; Figure 7F, black squares), none of the post-hoc tests were significant. There was also a significant main effect following treatment with ANI ($F(4,60) = 12.35, P < 0.0001$; Figure 7F, red circles). The decrease in the maximum rise slope from baseline values (401.56 ± 16.7 mV/ms) compared to 7 minutes post ANI (389.45 ± 16.6 mV/ms) was not significant, however it was significantly lower than baseline at 14 (363.57 ± 21.6 mV/ms, $P < 0.01$), 21 ($343.42 \pm 21.3, P < 0.01$), and 28 minutes ($343.04 \pm 22.5, P < 0.01$) post perfusion of ANI. These data are summarized in Table 2. Although the baseline measures across groups differ for both the spike height and the maximum rise slope, it is unlikely that this explains the significant effects in ANI experiments. This is because within the control group, cells with relatively high or low values maintained similar values throughout the duration of the experiment.

The maximum decay slope is measured as the maximum slope during the decay phase of the action potential. There were no changes in this parameter in control ($F(4,28) = 2.23, P > 0.05$) or ANI treated cells ($F(4,60) = 2.21, P > 0.05$; data not shown).

ANI alters multi-spike characteristics in CA1 neurons

The number of action potentials generated during long (1 second) sweeps in which multiple spikes were consistently elicited (see raw traces in Figure 8A) were evaluated for multiple time points in both control (left) and ANI (right) perfusion conditions. There were no significant changes in control cells ($F(4,24) = 1.02, P > 0.05$; Figure 8B, black squares),

Table 2: Single action potential active membrane properties. Average threshold, spike height, spike-half width, and maximum rise slope for control and ANI treated cells. Results of overall ANOVAs are in the left column. If the ANOVA was significant, results of the *post-hoc* Tukey HSD tests, as compared to baseline, are shown below the average.

Threshold (mV)					
Control	Baseline	Control-7	Control-14	Control-21	Control-28
$F(4,28)=1.39,$ $P > 0.05$	-48.76 ± 0.8	-50.42 ± 0.8	-50.90 ± 0.9	-50.46 ± 1.0	-49.69 ± 1.6
ANI	Baseline	ANI-7	ANI-14	ANI-21	ANI-28
$F(4,76)=0.92,$ $P > 0.05$	-49.76 ± 0.9	-48.91 ± 1.1	-48.70 ± 1.3	-46.11 ± 3.2	-46.15 ± 3.2
Spike Amplitude (mV)					
Control	Baseline	Control-7	Control-14	Control-21	Control-28
$F(4,28)=1.50,$ $P > 0.05$	109.47 ± 3.4	108.75 ± 3.5	107.72 ± 4.2	107.85 ± 3.6	106.10 ± 4.5
ANI	Baseline	ANI-7	ANI-14	ANI-21	ANI-28
$F(4,76)=16.48,$ $P < 0.0001$	112.92 ± 1.0	111.76 ± 1.3 <i>NS</i>	109.81 ± 1.2 $P < 0.01$	107.83 ± 1.3 $P < 0.01$	106.69 ± 1.6 $P < 0.01$
Half-Width (ms)					
Control	Baseline	Control-7	Control-14	Control-21	Control-28
$F(4,28)=1.45,$ $P > 0.05$	0.97 ± 0.4	0.95 ± 0.4	1.01 ± 0.5	1.03 ± 0.5	1.00 ± 0.5
ANI	Baseline	ANI-7	ANI-14	ANI-21	ANI-28
$F(4,76)=1.42,$ $P > 0.05$	0.77 ± 0.2	0.78 ± 0.2	0.84 ± 0.3	0.83 ± 0.2	0.78 ± 0.2
Maximum Rise Slope (mV/ms)					
Control	Baseline	Control-7	Control-14	Control-21	Control-28
$F(4,28)=3.09,$ $P < 0.05$	312.5 ± 33.9	$313.87 \pm$ 35.8 <i>NS</i>	$314.06 \pm$ 38.3 <i>NS</i>	$293.75 \pm$ 42.7 <i>NS</i>	$288.48 \pm$ 41.2 <i>NS</i>
ANI	Baseline	ANI-7	ANI-14	ANI-21	ANI-28
$F(4,60)=12.35,$ $P < 0.0001$	$401.56 \pm$ 16.7	$389.45 \pm$ 16.6 <i>NS</i>	$363.57 \pm$ 21.6 $P < 0.01$	$343.42 \pm$ 21.3 $P < 0.01$	$343.04 \pm$ 22.5 $P < 0.01$

Figure 8: Effect of ANI on other spiking characteristics. **A.** Raw data showing long (1 second) current sweeps in which multiple action potentials were elicited at time points equivalent to control (black), ANI (red), and post-ANI (gray) conditions in control (left) and ANI treated cells (right). Insets are an expansion showing the medium after-hyperpolarization (mAHP) during the same conditions. **B.** There was a trend toward an increase in the number of spikes elicited in control cells, although there were no significant changes (black squares, left). There was no significant change from baseline in the number of spikes elicited in ANI treated cells either 7 or 14 minutes following ANI application, however, there was a significant decrease at 21 and 28 minutes following ANI application. **C** The number of spikes elicited in control (black squares, left) cells is significantly greater than in ANI (red circles, right) cells across three incremental intensities. **D.** There were no significant changes in the difference between the first and last spike in the action potential train in control cells. In ANI cells, there was a significant increase in this difference 21 and 28 minutes following the addition of ANI. **E.** There were no significant changes in the average medium after-hyperpolarization in control cells (black squares, left). The increase in the mAHP 7 minutes following ANI application is not significantly different from baseline, however, it is significantly increased at 14, 21, and 28 minutes following ANI. Note that the mAHP is a negative value and an increase in its size appears as a decrease in graphical form.

although there was a slight increase on average. There was a significant net reduction across all time points, however, in ANI treated cells ($F(4,60) = 3.36, P < 0.05$; Figure 8B, red circles). This decrease from baseline (26.29 ± 1.4 spikes) in ANI cells was only significant at 21 (21.88 ± 1.4 spikes, $P < 0.05$) and 28 minutes (22.06 ± 1.6 spikes, $P < 0.05$) post-ANI in post-hoc tests. The spike frequency was also compared between baseline and ANI-21 for three increasing levels of current intensities (Figure 8C). A two-way repeated measures ANOVA revealed a main effect for condition (control vs. ANI; $F(1,21) = 5.99, P < 0.05$), reflecting a significant decrease for ANI-treated cells.

Although there was no significant difference in the half-width of single spikes or the first spike in a train, we sought to investigate if there was a change in the difference between the first and last spike of the train in ANI treated cells, as compared to control cells (half-width difference, Figure 8D). These data are summarized in Table 3.

The medium after-hyperpolarization (mAHP) was measured as the peak height of the voltage deflection from baseline following the termination of a depolarizing current sweep (1 second in duration) for which multiple spikes were elicited (see raw traces in the inset in Figure 8A). There were no significant changes in the mAHP of control cells over time ($F(4,24) = 0.89, P > 0.05$; Figure 8E, black squares), while there was a significant effect for ANI treated cells ($F(4,60) = 6.78, P < 0.001$; Figure 8E, red circles). There was no significant difference of the mAHP 7 minutes following ANI (-1.99 ± 0.3 mV) as compared to baseline (-1.47 ± 0.3 mV), however, the increase in the mAHP reached significance at 14 (-2.33 ± 0.3 mV, $P < 0.05$), 21 (-2.56 ± 0.3 mV, $P < 0.01$), as well as at 28 (-2.73 ± 0.4 mV, $P < 0.01$) minutes following the addition of ANI.

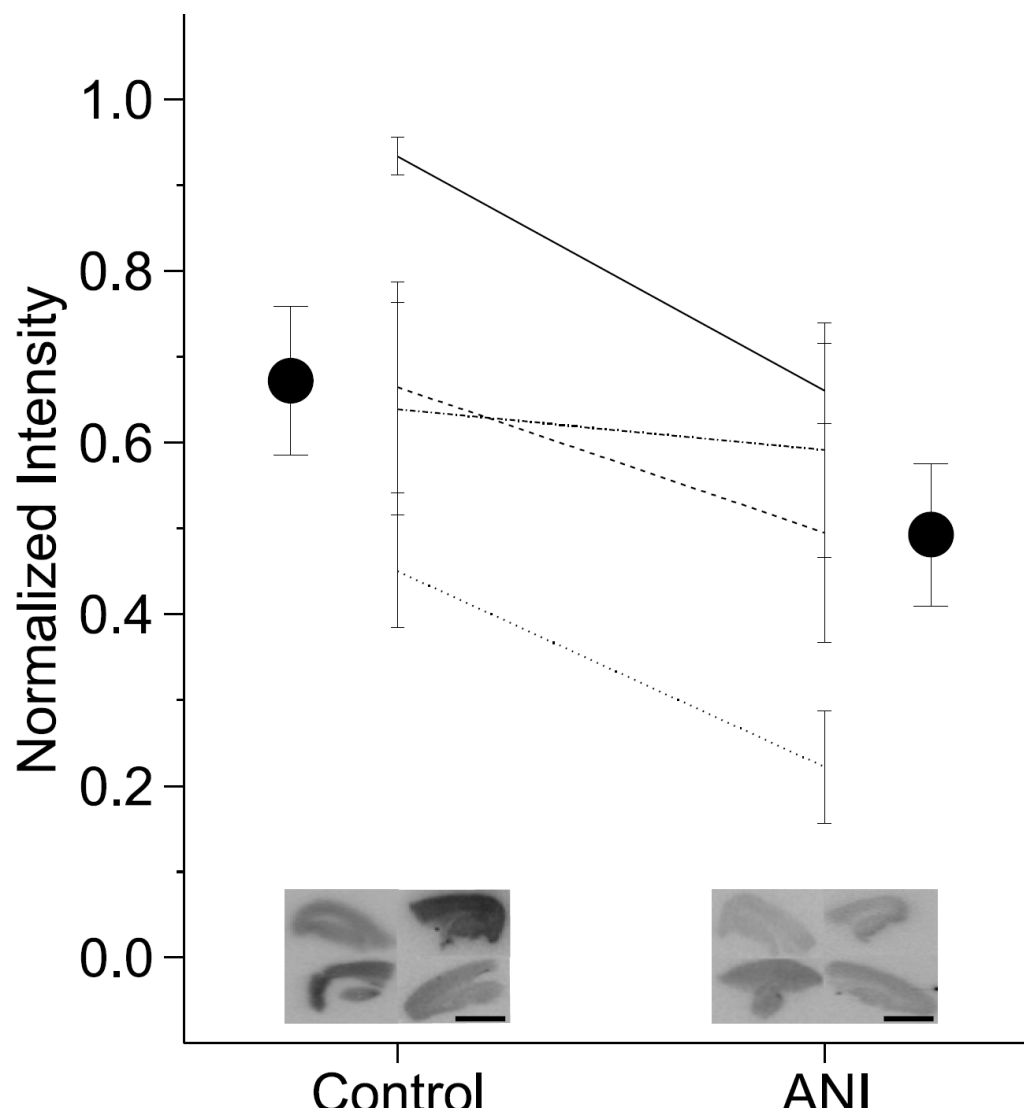
Table 3: Multiple Spike Properties. Average number of spikes elicited, medium after-hyperpolarization, and half-width difference for control and ANI treated cells. Results of overall ANOVAs are in the left column. If the ANOVA was significant, results of the *post-hoc* Tukey HSD tests, as compared to baseline, are shown below the average.

Number of Spikes Elicited					
Control	Baseline	Control-7	Control-14	Control-21	Control-28
$F(4,20)=1.34,$ $P > 0.05$	24.29 ± 2.2	29.00 ± 4.5	29.86 ± 5.6	32.00 ± 7.8	32.86 ± 7.8
ANI	Baseline	ANI-7	ANI-14	ANI-21	ANI-28
$F(4,60)=3.63,$ $P < 0.05$	26.29 ± 1.4	22.94 ± 1.7 <i>NS</i>	22.88 ± 1.5 <i>NS</i>	21.88 ± 1.4 $P < 0.05$	22.06 ± 1.6 $P < 0.05$
Medium After-Hyperpolarization (mV)					
Control	Baseline	Control-7	Control-14	Control-21	Control-28
$F(4,24)=0.89,$ $P > 0.05$	-1.32 ± 0.2	-1.05 ± 0.2	-1.53 ± 0.3	-1.45 ± 0.3	-1.19 ± 0.3
ANI	Baseline	ANI-7	ANI-14	ANI-21	ANI-28
$F(4,60)=6.78,$ $P < 0.001$	-1.47 ± 0.3	-1.99 ± 0.3 <i>NS</i>	-2.33 ± 0.3 $P < 0.05$	-2.56 ± 0.3 $P < 0.01$	-2.73 ± 0.4 $P < 0.01$
Half-Width Difference (ms)					
Control	Baseline	Control-7	Control-14	Control-21	Control-28
$F(4,24)=0.86,$ $P > 0.05$	0.63 ± 0.2	0.73 ± 0.2	0.94 ± 0.2	0.86 ± 0.2	1.04 ± 0.3
ANI	Baseline	ANI-7	ANI-14	ANI-21	ANI-28
$F(4,60)=7.42,$ $P < 0.0001$	0.57 ± 0.1	0.96 ± 0.1	1.07 ± 0.1	1.67 ± 0.3 $P < 0.01$	1.42 ± 0.2 $P < 0.01$

ANI reduces mitochondrial activity as evidenced by a decrease in TTC staining

In order to test if mitochondrial activity is affected by exposure to ANI, triphenyltetrazolium chloride (TTC) staining was used. Average light intensity values were calculated in the same manner as for autoradiography. As shown in Figure 9, there was a significant decrease in the amount of TTC staining in ANI treated cells (0.49 ± 0.8) from control slices (0.67 ± 0.9 , $P < 0.05$). Representative control and ANI slices are also shown in Figure 9 (inset).

Figure 9: Anisomycin impairs mitochondrial activity. Average (outside scatter points) and individual (inside lines) experiments showing a decrease in the normalized intensity of TTC staining in hippocampal slices treated with 100 μ M ANI for 30 minutes (0.86 ± 0.02), as compared to control slices (0.48 ± 0.05 , $P < 0.01$). A darker stain indicates more mitochondrial activity, and a higher normalized intensity. Example slices are shown for control and ANI (inset). Inset are four example transverse hippocampal slices used in each of the conditions. Scale bar corresponds to 4 mm.



Discussion

The results of the current study add to the growing literature which continues to cast doubt regarding the use of PSIs to test the *de novo* protein synthesis hypothesis. This hypothesis states that newly translated proteins are required for the formation of long-term memories (Davis and Squire, 1984). The most damning issue with this assumption is that it does not take into account the findings of memory recovery (Lattal and Abel, 2004), changes in neurotransmitter release (Canal et al., 2007; Qi and Gold, 2009), and arguably most importantly, alterations in neural activity (Sharma et al., 2012) and subsequent online processing (Greenberg et al., 2014; Dubue et al., 2015) following intracranial delivery of PSIs. Given our prior work showing impairments of neural activity and function, it was important to understand how PSIs, and in particular ANI, might operate at a cellular level to suppress neural signaling.

Electrophysiological properties of CA1 pyramidal neurons

The baseline electrophysiological properties of CA1 neurons reported in this study were consistent with previous work. Using whole-cell patch clamp recordings in transverse hippocampal slices (and similar aCSF and intracellular solutions), CA1 pyramidal neurons typically have resting membrane potentials between -60 and -70 mV (Staff et al., 2000). The threshold for firing action potentials generally requires an approximately 20 mV of depolarization, with spikes being elicited between -50 and -40 mV (Spruston and Johnston, 1992; Staff et al., 2000). These spikes generally reach a peak of 40 to 50 mV, giving them amplitudes between 80 and 100 mV (Scammell et al., 2003). Our control experiments (with baseline RMP of approximately -69 mV, threshold of approximately -49 mV, and spike amplitude of approximately 111 mV; Table 1,2) are consistent with these previously found

values. The finding that there were no significant changes in any properties measured in control cells over the duration of the experiments (lasting at least 30 minutes) suggest that the effects we observed were specific to ANI treatment and not cell rundown.

The membrane effects of ANI are consistent with mitochondrial dysfunction

The electrophysiological changes that were observed in the current study, a depolarization of the membrane with no change in input resistance or membrane time constant, and a decreased ability of cells to sustain healthy firing of action potentials led us to hypothesize that ANI may be exerting its neurosuppressive effects, either partially or fully, through the disruption of neural mitochondria. Indeed, the protein synthesis inhibitors emetine and cycloheximide have been previously shown to decrease mitochondrial membrane potential in cultured nerve cells (Hillefors et al., 2007). The same study found that emetine, but not cycloheximide, decreased basal ATP levels. Furthermore, both substances significantly impaired the ability of mitochondria to regenerate ATP levels following depolarization (Hillefors et al., 2007). A disruption of the sodium/potassium pump as a result of an inability to regenerate ATP levels would explain a reduction of membrane potential in the absence of changes to other passive membrane properties such as input resistance and tau. Furthermore, we would also expect to see a decrease in the spike peak, an increase in the rise slope of the AP, and a decreased ability to sustain AP firing in this case, all of which were observed in the current study (Figure 7-8).

Following the return of ANI free aCSF, there was no subsequent return of any of the measured properties to baseline values. We feel that this is likely consistent with the pharmacological profile action of ANI on protein synthesis.

Consistent with this hypothesis, we also observed a significant reduction in TTC staining following a 30 minute exposure of ANI to hippocampal slices, as compared with controls (Figure 9). The conversion of white TTC to 1,3,5-triphenylformazan, which is red in colour, is indicative of cellular respiration, as this conversion is dependent on electron transport (Riepe et al., 1996).

It is likely that the effects of ANI on mitochondria *in vivo* are more detrimental than is observed in the current patch clamp experiments. This is because the intracellular solution supplements the cell with an additional 3 mM of MgATP. *In vivo*, a disruption in mitochondria would lead to a rundown of ATP, which is required for long-lasting modulation of ion channels (Levitan, 1985).

In the future it would be useful to investigate this further by examining and comparing the effects of drugs such as chloramphenicol (inhibitor of mitochondrial respiration; (Moulin-Sallanon et al., 2005), antimycin a (inhibits ATP production; (Moulin-Sallanon et al., 2005), and ouabain (sodium/potassium pump inhibitor; (Moller et al., 1990) on global neural activity, as well as single cell membrane properties. It would be of particular interest to investigate how varying concentrations of these drugs, as well as ANI, affect neuronal membrane properties when applied via the intracellular solution. In this way, the effects of these modulators on post-synaptic effects could be studied at varying concentrations.

Effects of ANI on multiple spiking characteristics

Not only did ANI cause a decrease in the number of spikes elicited (Figure 8B) and corresponding spike frequencies at three intensity levels (Figure 8C), but also caused a disruption in the ability of ANI treated cells to maintain healthy firing throughout the train (Figure 8A).

Indeed, the difference in the half-width of spikes at the end of the train, as compared to the first spike, was significantly larger after ANI treatment (Figure 8D). This shows that ANI makes it difficult for cells to maintain consistent firing over a period of one second.

Another pertinent observation was an increase in the mAHP over time in ANI-treated but not control cells (Figure 8E). Based on our experiments it is unclear how ANI may be producing this increase in the mAHP.

Inhibition of protein synthesis in hippocampal slices

The observation that a 30 minute application of 100 μ M ANI was sufficient to significantly inhibit amino acid incorporation (Figure 5) is consistent with the hypothesis that the effects we have observed on neuronal membrane properties in the same preparation are due to the actual inhibition of protein synthesis. Indeed, suppression of neural activity *in vivo* following intracerebral delivery of ANI and cycloheximide was found not to be correlated to the concentration of the drug *per se*, but to the actual level of protein synthesis inhibition (Sharma et al., 2012). Furthermore, another study looking at the effects of synaptic activation on LTP found that the requirement for protein synthesis on LTP was dependent on synaptic stimulation (Fonseca et al., 2006). This study also showed that depending on the level of synaptic activation, PSI administration could disrupt early-LTP as well as maintenance of late-LTP. Most *in vitro* studies looking at the effects of protein synthesis inhibition on LTP use a much lower concentration (20-25 μ M) of ANI (Frey et al., 1988; Frey and Morris, 1997; Sajikumar and Frey, 2003; Fonseca et al., 2006) than *in vivo* studies looking at the effects of ANI on memory (226 to 452 mM; (Wanisch and Wotjak, 2008). While a 20 μ M bath application of ANI for 60 minutes has been shown to inhibit protein synthesis by up to 85% (Frey et al., 1988), this observation has

not been replicated. In our hands, a 30 minute application of 100 μ M inhibited protein synthesis by approximately 45% and was sufficient to disrupt single cell electrophysiological measures.

Effect of protein synthesis inhibition on other cell types

Although it has not been assessed directly, it is likely that the application of global protein synthesis inhibitors such as ANI would have effects on the functioning of glial cells as well as neurons. Neuronal-glia interactions are important for many aspects of neural activity including conduction of action potentials, synaptic transmission, and processing of information (Fields and Stevens-Graham, 2002). Indeed, astrocytes are thought to play a role in the maintenance of LTP as there is an increase in the surface density and a closer position of astrocytic processes to dendritic spines, terminal buttons, and the synaptic cleft following LTP induction (Wenzel et al., 1991).

Neurons are also reliant on astrocytes for the production of the neurotransmitter glutamate (Hertz and Zielke, 2004) as well as the regulation of glycogen breakdown and lactate release (Suzuki et al., 2011), both of which are important for neural function. These cells also play a role in the regulation of AMPA receptor density post-synaptically through the release of gliotransmitters (Bains and Oliet, 2007). As the above data suggests, glial cell activity is imperative for proper neuronal functioning, and consequentially learning and memory. It would therefore be of future interest to study the effects of protein synthesis inhibition on glial cells directly.

Effects of targeted molecular manipulations on neural activity

Manipulating the molecular activity of neurons in ways other than inhibition of protein synthesis can also have myriad effects on neuronal signalling. The transcriptional upregulation of

cyclic adenosine monophosphate (cAMP)-responsive element binding protein (CREB), which itself is a transcription factor for genes associated with synaptic plasticity and memory (Benito and Barco, 2010), is known to enhance membrane excitability (Dong et al., 2006; Han et al., 2006; Lopez de Armentia et al., 2007). It is presumed that this enhancement, due to a variety of potential changes in intrinsic membrane properties (Benito and Barco, 2010), is why transfected amygdalar neurons show a preponderance for being incorporated in a fear memory trace (Han et al., 2007; Viosca et al., 2009; Zhou et al., 2009). Conversely, inhibiting CREB reduces neural excitability and correspondingly, synaptic plasticity (Bourtchuladze et al., 1994; Dong et al., 2006; Han et al., 2006; Jancic et al., 2009; Zhou et al., 2009). What these findings indicate is that the manipulation of CREB activity may not in itself modulate memory *per se*, but may instead influence neuronal activity which in turn modulates memory induction and expression. Further evidence of activity-dependent effects have been shown for antisense (translational) inhibition of specific neural proteins which include reducing network activity (Garcia-Osta et al., 2006), as well as depressing neuronal subtype-specific cellular activity, responsiveness to exogenous and endogenous excitatory input, and even the ability to be antidromically activated (Neumann et al., 1995).

Protein kinase M zeta (PKM ζ), an atypical isoform of protein kinase C, has emerged as a particularly important protein for learning and memory as its activity is increased following synaptic and behavioural plasticity (Klann et al., 1993; Sacktor et al., 1993; Ling et al., 2002; Sajikumar et al., 2005). Its over-expression leads to increased maintenance of memory (Drier et al., 2002; Shema et al., 2011), and its inhibition disrupts both LTP and LTM (see (Kwapis and Helmstetter, 2014) for review). Issues with this hypothesis have since emerged, however, with the finding that conditional and constitutive PKM ζ knock-out mice have intact LTP and memory,

that is inhibited by zeta inhibitory peptide (ZIP; (Lee et al., 2013; Volk et al., 2013). A recent study in our lab therefore proposed that like global protein synthesis inhibitors, the effect of ZIP may be due to the inhibition of neural activity. Convincingly, ZIP was found to inhibit neural activity as strongly, and lasted even longer than the sodium channel blocker lidocaine (LeBlancq et al., *under review*).

Effects of alterations of neural activity on memory

The observation that ANI detrimentally disrupts neural activity is of particular importance, as this could explain its amnesic effects. The temporal firing dynamics of populations of neurons have substantial support for mediating the consolidation process of memory. The slow oscillation (SO) occurs during slow-wave sleep and groups cellular activity through periods of activity and silence (Buzsaki and Draguhn, 2004; Wolansky et al., 2006). In this way, locally generated fast rhythms important in synaptic plasticity such as gamma, thalamocortical spindles, and hippocampal ripples, can be temporally grouped (Dickson, 2010). In line with this, enhancement of SO improves previously encoded memories in both humans (Marshall et al., 2006; Ngo et al., 2013) and rats (Binder et al., 2013; Binder et al., 2014). Fast, large amplitude sharp waves occur during the SO and trigger fast (140-200 Hz) ripple oscillations (sharp-wave ripples; SPRs; (Buzsaki and Silva, 2012). Patterns of place cell firing that occur during the exploration of a novel environment are often repeated during SPRs in sleeping animals, suggesting a role in memory consolidation (Buzsaki, 1986; Skaggs and McNaughton, 1996; Carr et al., 2011). Indeed, SPRs occur more frequently following learning, and further increase in SPR occurrence have even been correlated to behavioural improvements in memory (Ramadan et al., 2009).

Changes in these fundamental patterns of neural activity following a period of learning can have profound effects on memory retrieval. Disruption of slow-wave sleep following learning has been shown to impair sleep-dependent increases in retention (Yaroush et al., 1971; Barrett and Ekstrand, 1972). Furthermore, when SPRs are selectively disrupted either during the learning process (Girardeau and Zugaro, 2011) or during post-learning sleep (Ego-Stengel and Wilson, 2010; Jadhav et al., 2012), spatial memory is impaired. Additionally, pharmacological inactivation of the hippocampus (Sacchetti et al., 1999; Daumas et al., 2005; Chang et al., 2008) or amygdala (Ledoux and Muller, 1997; Sacchetti et al., 1999) using sodium channel blockers, such as TTX and lidocaine, produces memory impairments in contextual fear conditioning paradigms.

In accordance with the idea that ANI induced amnesia is the result of blockage of neural activity, a recent paper showed that direct stimulation of the neurons involved in the encoding of the memory was sufficient to recovery the disrupted memory (Ryan et al., 2015). There were no observed changes in intrinsic cellular properties following bath application of ANI in this study, however, the concentration used was very low (40 μ M). Even with this low concentration, however, ANI was found to decrease AMPA/NMDA current ratios, spontaneous excitatory postsynaptic currents, and engram cell specific increases in spine density (Ryan et al., 2015).

Conclusions

Global protein synthesis inhibition, as well as targeted techniques, can have profound effects on neural activity sufficient to explain their effects on memory. The current study has expanded the effects of the global PSI ANI on membrane properties at the level of the single cell. In the future, caution should be used when making the leap from changes in molecular activity to

changes in behaviour, without examining what is going on at the level of network and cellular activity.

References

- Amaral DG, Witter MP (1989) The three-dimensional organization of the hippocampal formation: a review of anatomical data. *Neuroscience* 31:571-591.
- Andersen P, Bliss TV, Lomo T, Olsen LI, Skrede KK (1969) Lamellar organization of hippocampal excitatory pathways. *Acta physiologica Scandinavica* 76:4A-5A.
- Bains JS, Oliet SH (2007) Glia: they make your memories stick! *Trends in neurosciences* 30:417-424.
- Bannister NJ, Larkman AU (1995) Dendritic morphology of CA1 pyramidal neurones from the rat hippocampus: I. Branching patterns. *The Journal of comparative neurology* 360:150-160.
- Barondes SH, Cohen HD (1966) Puromycin effect on successive phases of memory storage. *Science (New York, NY)* 151:594-595.
- Barondes SH, Cohen HD (1968) Arousal and the conversion of "short-term" to "long-term" memory. *Proceedings of the National Academy of Sciences of the United States of America* 61:923-929.
- Barrett TR, Ekstrand BR (1972) Effect of sleep on memory. 3. Controlling for time-of-day effects. *Journal of experimental psychology* 96:321-327.
- Benito E, Barco A (2010) CREB's control of intrinsic and synaptic plasticity: implications for CREB-dependent memory models. *Trends in neurosciences* 33:230-240.
- Binder S, Rawohl J, Born J, Marshall L (2013) Transcranial slow oscillation stimulation during NREM sleep enhances acquisition of the radial maze task and modulates cortical network activity in rats. *Frontiers in behavioral neuroscience* 7:220.
- Binder S, Berg K, Gasca F, Lafon B, Parra LC, Born J, Marshall L (2014) Transcranial Slow Oscillation Stimulation During Sleep Enhances Memory Consolidation in Rats. *Brain stimulation*.
- Bourtchuladze R, Frenguelli B, Blendy J, Cioffi D, Schutz G, Silva AJ (1994) Deficient long-term memory in mice with a targeted mutation of the cAMP-responsive element-binding protein. *Cell* 79:59-68.
- Buzsaki G (1986) Hippocampal sharp waves: their origin and significance. *Brain research* 398:242-252.
- Buzsaki G, Draguhn A (2004) Neuronal oscillations in cortical networks. *Science (New York, NY)* 304:1926-1929.
- Buzsaki G, Silva FL (2012) High frequency oscillations in the intact brain. *Progress in neurobiology* 98:241-249.
- Canal CE, Chang Q, Gold PE (2007) Amnesia produced by altered release of neurotransmitters after intraamygdala injections of a protein synthesis inhibitor. *Proceedings of the National Academy of Sciences of the United States of America* 104:12500-12505.
- Carr MF, Jadhav SP, Frank LM (2011) Hippocampal replay in the awake state: a potential substrate for memory consolidation and retrieval. *Nature neuroscience* 14:147-153.
- Chang SD, Chen DY, Liang KC (2008) Infusion of lidocaine into the dorsal hippocampus before or after the shock training phase impaired conditioned freezing in a two-phase training task of contextual fear conditioning. *Neurobiology of learning and memory* 89:95-105.
- Cohen HD, Barondes SH (1966) Further studies of learning and memory after intracerebral actinomycin-D. *Journal of neurochemistry* 13:207-211.

- Cohen HD, Barondes SH (1967) Puromycin effect on memory may be due to occult seizures. *Science (New York, NY)* 157:333-334.
- Cohen HD, Ervin F, Barondes SH (1966) Puromycin and cycloheximide: different effects on hippocampal electrical activity. *Science (New York, NY)* 154:1557-1558.
- Cohen NJ, Squire LR (1980) Preserved learning and retention of pattern-analyzing skill in amnesia: dissociation of knowing how and knowing that. *Science (New York, NY)* 210:207-210.
- Dahl NA (1969) Nerve electrical activity; depression by puromycin not related to inhibited protein synthesis. *Journal of neurobiology* 1:169-180.
- Daumas S, Halley H, Frances B, Lassalle JM (2005) Encoding, consolidation, and retrieval of contextual memory: differential involvement of dorsal CA3 and CA1 hippocampal subregions. *Learning & memory (Cold Spring Harbor, NY)* 12:375-382.
- Davis HP, Squire LR (1984) Protein synthesis and memory: a review. *Psychological bulletin* 96:518-559.
- Davis HP, Spanis CW, Squire LR (1976) Inhibition of cerebral protein synthesis: performance at different times after passive avoidance training. *Pharmacology, biochemistry, and behavior* 4:13-16.
- Dickson CT (2010) Ups and downs in the hippocampus: the influence of oscillatory sleep states on "neuroplasticity" at different time scales. *Behavioural brain research* 214:35-41.
- Dong Y, Green T, Saal D, Marie H, Neve R, Nestler EJ, Malenka RC (2006) CREB modulates excitability of nucleus accumbens neurons. *Nature neuroscience* 9:475-477.
- Drier EA, Tello MK, Cowan M, Wu P, Blace N, Sacktor TC, Yin JC (2002) Memory enhancement and formation by atypical PKM activity in *Drosophila melanogaster*. *Nature neuroscience* 5:316-324.
- Dubue JD, McKinney TL, Treit D, Dickson CT (2015) Intrahippocampal anisomycin impairs spatial performance on the Morris water maze. *J Neurosci* 35:11118-11124.
- Dvorak-Carbone H, Schuman EM (1999) Patterned activity in stratum lacunosum moleculare inhibits CA1 pyramidal neuron firing. *Journal of neurophysiology* 82:3213-3222.
- Ego-Stengel V, Wilson MA (2010) Disruption of ripple-associated hippocampal activity during rest impairs spatial learning in the rat. *Hippocampus* 20:1-10.
- Fields RD, Stevens-Graham B (2002) New insights into neuron-glia communication. *Science (New York, NY)* 298:556-562.
- Flexner JB, Flexner LB (1967) Restoration of expression of memory lost after treatment with puromycin. *Proceedings of the National Academy of Sciences of the United States of America* 57:1651-1654.
- Flexner JB, Flexner LB (1970) Adrenalectomy and the suppression of memory by puromycin. *Proceedings of the National Academy of Sciences of the United States of America* 66:48-52.
- Flexner JB, Flexner LB, Stellar E (1963) Memory in mice as affected by intracerebral puromycin. *Science (New York, NY)* 141:57-59.
- Flexner LB, Goodman RH (1975) Studies on memory: inhibitors of protein synthesis also inhibit catecholamine synthesis. *Proceedings of the National Academy of Sciences of the United States of America* 72:4660-4663.
- Flexner LB, Serota RG, Goodman RH (1973) Cycloheximide and acetoxycycloheximide: inhibition of tyrosine hydroxylase activity and amnesic effects. *Proceedings of the National Academy of Sciences of the United States of America* 70:354-356.

- Flood JF, Bennett EL, Orme AE, Rosenzweig MR (1975) Effects of protein synthesis inhibition on memory for active avoidance training. *Physiology & behavior* 14:177-184.
- Fonseca R, Nagerl UV, Bonhoeffer T (2006) Neuronal activity determines the protein synthesis dependence of long-term potentiation. *Nature neuroscience* 9:478-480.
- Frey U, Morris RG (1997) Synaptic tagging and long-term potentiation. *Nature* 385:533-536.
- Frey U, Krug M, Reymann KG, Matthies H (1988) Anisomycin, an inhibitor of protein synthesis, blocks late phases of LTP phenomena in the hippocampal CA1 region in vitro. *Brain research* 452:57-65.
- Gambetti P, Gonatas NK, Flexner LB (1968) Puromycin: action on neuronal mitochondria. *Science (New York, NY)* 161:900-902.
- Garcia-Osta A, Tsokas P, Pollonini G, Landau EM, Blitzer R, Alberini CM (2006) MuSK expressed in the brain mediates cholinergic responses, synaptic plasticity, and memory formation. *J Neurosci* 26:7919-7932.
- Girardeau G, Zugaro M (2011) Hippocampal ripples and memory consolidation. *Current opinion in neurobiology* 21:452-459.
- Greenberg A, Ward-Flanagan R, Dickson CT, Treit D (2014) ANI inactivation: unconditioned anxiolytic effects of anisomycin in the ventral hippocampus. *Hippocampus* 24:1308-1316.
- Grollman AP (1966) Structural basis for inhibition of protein synthesis by emetine and cycloheximide based on an analogy between ipecac alkaloids and glutarimide antibiotics. *Proceedings of the National Academy of Sciences of the United States of America* 56:1867-1874.
- Grollman AP (1967) Inhibitors of protein biosynthesis. II. Mode of action of anisomycin. *The Journal of biological chemistry* 242:3226-3233.
- Han JH, Kushner SA, Yiu AP, Cole CJ, Matynia A, Brown RA, Neve RL, Guzowski JF, Silva AJ, Josselyn SA (2007) Neuronal competition and selection during memory formation. *Science (New York, NY)* 316:457-460.
- Han MH, Bolanos CA, Green TA, Olson VG, Neve RL, Liu RJ, Aghajanian GK, Nestler EJ (2006) Role of cAMP response element-binding protein in the rat locus ceruleus: regulation of neuronal activity and opiate withdrawal behaviors. *J Neurosci* 26:4624-4629.
- Hernandez PJ, Abel T (2008) The role of protein synthesis in memory consolidation: progress amid decades of debate. *Neurobiology of learning and memory* 89:293-311.
- Hertz L, Zielke HR (2004) Astrocytic control of glutamatergic activity: astrocytes as stars of the show. *Trends in neurosciences* 27:735-743.
- Hillefors M, Gioio AE, Mameza MG, Kaplan BB (2007) Axon viability and mitochondrial function are dependent on local protein synthesis in sympathetic neurons. *Cellular and molecular neurobiology* 27:701-716.
- Jadhav SP, Kemere C, German PW, Frank LM (2012) Awake hippocampal sharp-wave ripples support spatial memory. *Science (New York, NY)* 336:1454-1458.
- Jancic D, Lopez de Armentia M, Valor LM, Olivares R, Barco A (2009) Inhibition of cAMP response element-binding protein reduces neuronal excitability and plasticity, and triggers neurodegeneration. *Cereb Cortex* 19:2535-2547.
- Jay TM, Glowinski J, Thierry AM (1989) Selectivity of the hippocampal projection to the prelimbic area of the prefrontal cortex in the rat. *Brain research* 505:337-340.

- Kandel ER (2001) The molecular biology of memory storage: a dialog between genes and synapses. *Bioscience reports* 24:475-522.
- Kempainen S, Jolkkonen E, Pitkanen A (2002) Projections from the posterior cortical nucleus of the amygdala to the hippocampal formation and parahippocampal region in rat. *Hippocampus* 12:735-755.
- Klann E, Chen SJ, Sweatt JD (1993) Mechanism of protein kinase C activation during the induction and maintenance of long-term potentiation probed using a selective peptide substrate. *Proceedings of the National Academy of Sciences of the United States of America* 90:8337-8341.
- Kleim JA, Bruneau R, Calder K, Pocock D, VandenBerg PM, MacDonald E, Monfils MH, Sutherland RJ, Nader K (2003) Functional organization of adult motor cortex is dependent upon continued protein synthesis. *Neuron* 40:167-176.
- Krettek JE, Price JL (1977) The cortical projections of the mediodorsal nucleus and adjacent thalamic nuclei in the rat. *The Journal of comparative neurology* 171:157-191.
- Kwapis JL, Helmstetter FJ (2014) Does PKM(zeta) maintain memory? *Brain research bulletin* 105:36-45.
- Lattal KM, Abel T (2004) Behavioral impairments caused by injections of the protein synthesis inhibitor anisomycin after contextual retrieval reverse with time. *Proceedings of the National Academy of Sciences of the United States of America* 101:4667-4672.
- LeBlancq MJ, McKiney TL, Dickson CT (*under review*) ZIP it: Neural silencing is an additional effect of the PKM ζ inhibitor, zeta inhibitory peptide *J Neurosci*.
- Lechner HA, Squire LR, Byrne JH (1999) 100 years of consolidation--remembering Muller and Pilzecker. *Learning & memory* (Cold Spring Harbor, NY) 6:77-87.
- Ledoux JE, Muller J (1997) Emotional memory and psychopathology. *Philosophical transactions of the Royal Society of London* 352:1719-1726.
- Lee AM, Kanter BR, Wang D, Lim JP, Zou ME, Qiu C, McMahon T, Dadgar J, Fischbach-Weiss SC, Messing RO (2013) Prkcz null mice show normal learning and memory. *Nature* 493:416-419.
- Levitan IB (1985) Phosphorylation of ion channels. *The Journal of membrane biology* 87:177-190.
- Lewis FT (1923) The significance of the term *Hippocampus*. . *The Journal of comparative neurology* 35:213-230.
- Ling DS, Benardo LS, Serrano PA, Blace N, Kelly MT, Crary JF, Sacktor TC (2002) Protein kinase Mzeta is necessary and sufficient for LTP maintenance. *Nature neuroscience* 5:295-296.
- Lopez de Armentia M, Jancic D, Olivares R, Alarcon JM, Kandel ER, Barco A (2007) cAMP response element-binding protein-mediated gene expression increases the intrinsic excitability of CA1 pyramidal neurons. *J Neurosci* 27:13909-13918.
- Luttges MW, Andry DK, MacInnes JW (1972) Cycloheximide alters the neural and behavioral responses of mice to electroconvulsive shock. *Brain research* 46:411-416.
- Marshall L, Helgadottir H, Molle M, Born J (2006) Boosting slow oscillations during sleep potentiates memory. *Nature* 444:610-613.
- Matthews EA, Linardakis JM, Disterhoft JF (2009) The fast and slow afterhyperpolarizations are differentially modulated in hippocampal neurons by aging and learning. *J Neurosci* 29:4750-4755.

- McGaugh JL (1966) Time-dependent processes in memory storage. *Science (New York, NY)* 153:1351-1358.
- McGaugh JL (2000) Memory--a century of consolidation. *Science (New York, NY)* 287:248-251.
- Moller B, Vaag A, Johansen T (1990) Ouabain inhibition of the sodium-potassium pump: estimation of ED50 in different types of human leucocytes in vitro. *British journal of clinical pharmacology* 29:93-100.
- Moser MB, Rowland DC, Moser EI (2015) Place cells, grid cells, and memory. *Cold Spring Harbor perspectives in medicine* 5:a021808.
- Moulin-Sallanon M, Millet P, Rousset C, Zimmer L, Debilly G, Petit JM, Cespeglio R, Magistretti P, Ibanez V (2005) Chloramphenicol decreases brain glucose utilization and modifies the sleep-wake cycle architecture in rats. *Journal of neurochemistry* 93:1623-1632.
- Neher E (1992) Correction for liquid junction potentials in patch clamp experiments. *Methods in enzymology* 207:123-131.
- Neumann I, Kremarik P, Pittman QJ (1995) Acute, sequence-specific effects of oxytocin and vasopressin antisense oligonucleotides on neuronal responses. *Neuroscience* 69:997-1003.
- Ngo HV, Martinetz T, Born J, Molle M (2013) Auditory closed-loop stimulation of the sleep slow oscillation enhances memory. *Neuron* 78:545-553.
- Obrig TG, Culp WJ, McKeehan WL, Hardesty B (1971) The mechanism by which cycloheximide and related glutarimide antibiotics inhibit peptide synthesis on reticulocyte ribosomes. *The Journal of biological chemistry* 246:174-181.
- Oh MM, Kuo AG, Wu WW, Sametsky EA, Disterhoft JF (2003) Watermaze learning enhances excitability of CA1 pyramidal neurons. *Journal of neurophysiology* 90:2171-2179.
- Pestka S (1971) Inhibitors of ribosome functions. *Annual review of microbiology* 25:487-562.
- Pyapali GK, Sik A, Penttonen M, Buzsaki G, Turner DA (1998) Dendritic properties of hippocampal CA1 pyramidal neurons in the rat: intracellular staining in vivo and in vitro. *The Journal of comparative neurology* 391:335-352.
- Qi Z, Gold PE (2009) Intrahippocampal infusions of anisomycin produce amnesia: contribution of increased release of norepinephrine, dopamine, and acetylcholine. *Learning & memory (Cold Spring Harbor, NY)* 16:308-314.
- Ramadan W, Eschenko O, Sara SJ (2009) Hippocampal sharp wave/ripples during sleep for consolidation of associative memory. *PloS one* 4:e6697.
- Riepe MW, Niemi WN, Megow D, Ludolph AC, Carpenter DO (1996) Mitochondrial oxidation in rat hippocampus can be preconditioned by selective chemical inhibition of succinic dehydrogenase. *Experimental neurology* 138:15-21.
- Roberts RB, Flexner JB, Flexner LB (1970) Some evidence for the involvement of adrenergic sites in the memory trace. *Proceedings of the National Academy of Sciences of the United States of America* 66:310-313.
- Ryan TJ, Roy DS, Pignatelli M, Arons A, Tonegawa S (2015) Memory. Engram cells retain memory under retrograde amnesia. *Science (New York, NY)* 348:1007-1013.
- Sacchetti B, Lorenzini CA, Baldi E, Tassoni G, Bucherelli C (1999) Auditory thalamus, dorsal hippocampus, basolateral amygdala, and perirhinal cortex role in the consolidation of conditioned freezing to context and to acoustic conditioned stimulus in the rat. *J Neurosci* 19:9570-9578.

- Sacktor TC, Osten P, Valsamis H, Jiang X, Naik MU, Sublette E (1993) Persistent activation of the zeta isoform of protein kinase C in the maintenance of long-term potentiation. *Proceedings of the National Academy of Sciences of the United States of America* 90:8342-8346.
- Sajikumar S, Frey JU (2003) Anisomycin inhibits the late maintenance of long-term depression in rat hippocampal slices in vitro. *Neuroscience letters* 338:147-150.
- Sajikumar S, Navakkode S, Sacktor TC, Frey JU (2005) Synaptic tagging and cross-tagging: the role of protein kinase Mzeta in maintaining long-term potentiation but not long-term depression. *J Neurosci* 25:5750-5756.
- Scammell TE, Arrigoni E, Thompson MA, Ronan PJ, Saper CB, Greene RW (2003) Focal deletion of the adenosine A1 receptor in adult mice using an adeno-associated viral vector. *J Neurosci* 23:5762-5770.
- Schwartz JH, Castellucci VF, Kandel ER (1971) Functioning of identified neurons and synapses in abdominal ganglion of *Aplysia* in absence of protein synthesis. *Journal of neurophysiology* 34:939-953.
- Scoville WB, Milner B (1957) Loss of recent memory after bilateral hippocampal lesions. *Journal of neurology, neurosurgery, and psychiatry* 20:11-21.
- Serota RG, Roberts RB, Flexner LB (1972) Acetoxycycloheximide-induced transient amnesia: protective effects of adrenergic stimulants. *Proceedings of the National Academy of Sciences of the United States of America* 69:340-342.
- Sharma AV, Nargang FE, Dickson CT (2012) Neurosilence: profound suppression of neural activity following intracerebral administration of the protein synthesis inhibitor anisomycin. *J Neurosci* 32:2377-2387.
- Shema R, Haramati S, Ron S, Hazvi S, Chen A, Sacktor TC, Dudai Y (2011) Enhancement of consolidated long-term memory by overexpression of protein kinase Mzeta in the neocortex. *Science (New York, NY)* 331:1207-1210.
- Skaggs WE, McNaughton BL (1996) Replay of neuronal firing sequences in rat hippocampus during sleep following spatial experience. *Science (New York, NY)* 271:1870-1873.
- Spruston N, Johnston D (1992) Perforated patch-clamp analysis of the passive membrane properties of three classes of hippocampal neurons. *Journal of neurophysiology* 67:508-529.
- Squire LR, Barondes SH (1972) Variable decay of memory and its recovery in cycloheximide-treated mice. *Proceedings of the National Academy of Sciences of the United States of America* 69:1416-1420.
- Squire LR, Barondes SH (1973) Memory impairment during prolonged training in mice given inhibitors of cerebral protein synthesis. *Brain research* 56:215-225.
- Squire LR, Stark CE, Clark RE (2004) The medial temporal lobe. *Annual review of neuroscience* 27:279-306.
- Staff NP, Jung HY, Thiagarajan T, Yao M, Spruston N (2000) Resting and active properties of pyramidal neurons in subiculum and CA1 of rat hippocampus. *Journal of neurophysiology* 84:2398-2408.
- Stern SA, Alberini CM (2013) Mechanisms of memory enhancement. *Wiley interdisciplinary reviews* 5:37-53.
- Suzuki A, Stern SA, Bozdagi O, Huntley GW, Walker RH, Magistretti PJ, Alberini CM (2011) Astrocyte-neuron lactate transport is required for long-term memory formation. *Cell* 144:810-823.

- Tamamaki N, Abe K, Nojyo Y (1987) Columnar organization in the subiculum formed by axon branches originating from single CA1 pyramidal neurons in the rat hippocampus. *Brain research* 412:156-160.
- Tombaugh GC, Rowe WB, Rose GM (2005) The slow afterhyperpolarization in hippocampal CA1 neurons covaries with spatial learning ability in aged Fisher 344 rats. *J Neurosci* 25:2609-2616.
- van Groen T, Wyss JM (1990) Extrinsic projections from area CA1 of the rat hippocampus: olfactory, cortical, subcortical, and bilateral hippocampal formation projections. *The Journal of comparative neurology* 302:515-528.
- Viosca J, Lopez de Armentia M, Jancic D, Barco A (2009) Enhanced CREB-dependent gene expression increases the excitability of neurons in the basal amygdala and primes the consolidation of contextual and cued fear memory. *Learning & memory (Cold Spring Harbor, NY)* 16:193-197.
- Volk LJ, Bachman JL, Johnson R, Yu Y, Haganir RL (2013) PKM-zeta is not required for hippocampal synaptic plasticity, learning and memory. *Nature* 493:420-423.
- Wanisch K, Wotjak CT (2008) Time course and efficiency of protein synthesis inhibition following intracerebral and systemic anisomycin treatment. *Neurobiology of learning and memory* 90:485-494.
- Wenzel J, Lammert G, Meyer U, Krug M (1991) The influence of long-term potentiation on the spatial relationship between astrocyte processes and potentiated synapses in the dentate gyrus neuropil of rat brain. *Brain research* 560:122-131.
- Wilcox GL, Jr., Andry DK, Luttges MW (1974) Cycloheximide effects on electroencephalographic and evoked responses in mice. *Behavioral biology* 12:81-92.
- Witter MP, Griffioen AW, Jorritsma-Byham B, Krijnen JL (1988) Entorhinal projections to the hippocampal CA1 region in the rat: an underestimated pathway. *Neuroscience letters* 85:193-198.
- Witter MP, Wouterlood FG, Naber PA, Van Haeften T (2000) Anatomical organization of the parahippocampal-hippocampal network. *Annals of the New York Academy of Sciences* 911:1-24.
- Wolansky T, Clement EA, Peters SR, Palczak MA, Dickson CT (2006) Hippocampal slow oscillation: a novel EEG state and its coordination with ongoing neocortical activity. *J Neurosci* 26:6213-6229.
- Wouterlood FG, Saldana E, Witter MP (1990) Projection from the nucleus reuniens thalami to the hippocampal region: light and electron microscopic tracing study in the rat with the anterograde tracer Phaseolus vulgaris-leucoagglutinin. *The Journal of comparative neurology* 296:179-203.
- Yaroush R, Sullivan MJ, Ekstrand BR (1971) Effect of sleep on memory. II. Differential effect of the first and second half of the night. *Journal of experimental psychology* 88:361-366.
- Zhou Y, Won J, Karlsson MG, Zhou M, Rogerson T, Balaji J, Neve R, Poirazi P, Silva AJ (2009) CREB regulates excitability and the allocation of memory to subsets of neurons in the amygdala. *Nature neuroscience* 12:1438-1443.